Removal of Organic Micro-pollutants Present in the Effluent of Wastewater Treatment Plant by Zeolite Granules

Shan Jiang

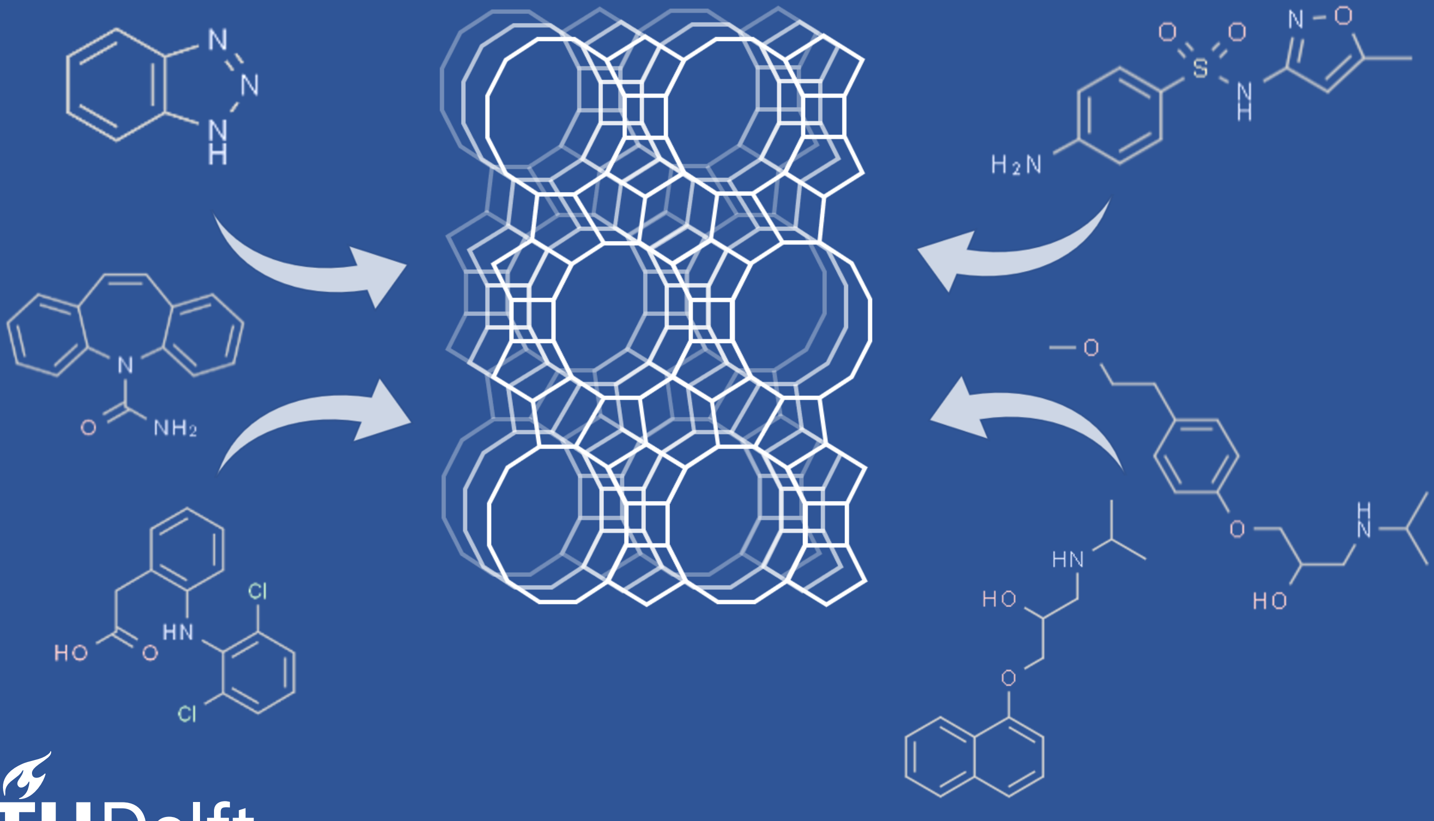

Removal of Organic Micro-pollutants Present in the Effluent of Wastewater Treatment Plant by Zeolite Granules

by

Shan Jiang

to obtain the degree of
Master of Science in Civil Engineering (Track of Environmental Engineering)
at the Delft University of Technology.

Student number:	5045452	
Project duration:	January 1, 2021 – January 10, 2021	
Thesis committee:	Prof. Dr. ir. L.C. Rietveld,	TU Delft, chair
	Dr. ir. S.G.J. Heijman,	TU Delft, supervisor
	Prof. Dr. ir. Jules van Lier,	TU Delft
	Dr. ir. Nan Jiang,	TU Delft, daily-supervisor

TU Delft

Preface

This article reports my master thesis work "Removal of organic micro-pollutants present in the effluent of wastewater treatment plant by zeolite granules". The experimental part was conducted in water lab under the supervision of Dr. Bas Heijman and Dr. Nan Jiang.

I would like to sincerely thank my supervisor Bas Heijman for his excellent guidance and supports during the thesis process. I also wish to thank Luuk Rietveld and Jules van Lier for their valuable suggestions to improve my report. I want to express special thanks to my daily supervisor Nan Jiang, for her advice in completing systematical scientific research. I also want to thank to Mingyan Fu for providing me with suggestions on the experimental design and the prediction model implement. I gratefully thank my classmates in environmental engineering and water management. We had a short but enjoyable study time on campus before the COVID-19 outbreak. In 2021, the lab work made us see each other in the lab and share our thesis progress and daily life.

Last but not least, I thank my boyfriend for his company in the Netherlands during the COVID-19 pandemic and for supporting me through the difficult time. I am grateful for the company of my lovely cat Cookie. It always slept on my lap or by my table when I was working at home. I express my gratitude and love to my parents for their unconditional support and encouragement.

I will never forget the shining days in TU Delft. The memories of this journey in the Netherlands will be cherished forever in my life.

Shan Jiang
December 2021
Rotterdam

Abstract

Zeolites can be used for the adsorption of organic micropollutants (OMPs) from water. In this research, the potential applications of zeolite granules for OMP removal in wastewater treatment plants (WWTPs) were discovered. The adsorption of 18 target OMPs by zeolite granules was fully studied in batch and column experiments. The adsorption capacity and kinetics of OMPs in demineralised water (DW) and secondary effluent from WWTP (WW matrix) were investigated. A prediction model of OMP breakthrough curves in zeolite packed columns was established and evaluated.

It was found that the adsorption of OMPs by zeolite granules in batch and column experiments was influenced by OMP species, water matrices and operational parameters (e.g., superficial velocity and contact time). Positively charged OMPs were better adsorbed by zeolite granules than neutral and negatively charged OMPs. In most cases, the adsorption capacity and kinetics of OMPs were reduced in WW matrix, which led to an earlier breakthrough in columns. On the contrary, WW matrix enhanced the adsorption capacity and kinetics of a few negatively charged OMPs, such as diclofenac and clofibric acid. Higher zeolite dosage resulted in faster OMP adsorption kinetics.

Column experiments showed that 12 of the 18 target OMPs could be effectively removed at the EBCT of 12 min, achieving removal efficiencies of 50% over 10 days. The mathematic model for the prediction of OMP breakthrough curves was optimized by applying larger kinetic constants obtained from the batch experiment. It was predicted an EBCT of 15 min is an alternative for a 7-day operation to remove OMPs sufficiently by zeolite packed columns.

Contents

List of Figures

List of Tables

List of abbreviations

AOP	Advanced oxidation process
BD	Bed depth
DOC	Dissolved organic carbon
DOM	Dissolved organic matter
DW	Demineralised water
EBCT	Empty bed contact time
EC	Electrical conductivity
FD	Fickian diffusion
I&W	Ministry of Infrastructure and Water Management
IC	Ion chromatography
IPD	Intra-particle diffusion
LC–MS	Liquid chromatography–mass spectrometry
LDF	Linear driving force
MBR	Membrane bioreactor
NOM	Natural organic matter
PFO	Pseudo-first-order
PPCP	Pharmaceuticals and personal care product
PSO	Pseudo-second-order
QDF	Quadratic driving force
TOC	Total organic carbon
UVT	UV transmittance
WW	Wastewater
WWTP	Wastewater treatment plant

1

Introduction

1.1. Occurrence and treatment of OMPs

With the development of industry and economy, the production of synthesis chemicals increases and the containments enter the aquatic environment inevitably via different flow paths. Organic micro-pollutants (OMPs) are defined as anthropogenic chemicals with low concentrations ranging from ng/L up to μg/L levels in water bodies (Eggen et al., 2014). Due to their ecotoxicological potential, OMPs are of growing concern.

OMPs which can be detected in the European aquatic environment can be classed into more than 20 categories, including pharmaceuticals and personal care products (PPCPs), pesticides, and industrial chemicals (Arslan et al., 2017). The wastewater (WW) from agriculture, industry and households is the major pollutant source of OMPs. Some research studied the presence of OMPs in European existing wastewater treatment plants (WWTPs) and the natural water environment. Loos et al. (2013) analyzed 156 micropollutants in effluents of 90 European WWTPs. The average contents of OMPs in the effluents were 2.9 μg/L for methyl-benzotriazole, 6.3 μg/L for benzotriazole, 229 ng/L for trimethoprim, 191 ng/L for caffeine, 832 ng/L for carbamazepine, 49.5 ng/L for diclofenac, 280 ng/L for sulfamethoxazole, 86.0 ng/L for ketoprofen, 5.3 ng/L for clofibric acid. Rodriguez-Mozaz et al. (2020) studied 53 antibiotic residues in WWTP effluents of 7 European countries. The ranges of antibiotics in effluents were 4.5-313.2 ng/L for clarithromycin, 7.1-123.4 ng/L for sulfamethoxazole and 15.2-190.6 ng/L for trimethoprim. Gabet-Giraud et al. (2014) analyzed beta blockers in French WWTPs effluents with the median concentration of 38 ng/L for metoprolol, 138 ng/L for propranolol, and 435 ng/L for sotalol. Datel and Hrabankova (2020) obtained maximum concentrations of PPCPs in raw water from the Svihov reservoir, which were 58 ng/L for diclofenac, 157 ng/L for gabapentin, 99 ng/L for hydrochlorothiazide.

In Europe, a watch list of substances for Union-wide monitoring in the field of water policy was established in the Commission Implementing Decision 2008/105/EU (Commission, 2008). Decision 2015/10495/EU (Commission, 2015) and Decision 2018/840/EU (Commission, 2018) updated the watch list including some pharmaceuticals, like diclofenac. The watch list showed that monitoring of these substances was necessary and should be given particular consideration. In the Netherlands, the Ministry of Infrastructure and Water Management (I&W) is searching for innovative technologies to remove OMPs from WWTPs.

To deal with amounts of municipal WW, current WWTPs are not exclusively designed to remove most OMPs. The levels of OMPs with potential threats can be detected in the effluents of WWTPs since the removal of OMPs in the biological treatment process is limited. Di Marcantonio et al. (2020) compared the concentrations of 13 OMPs in the influent and effluent of 76 full-scale WWTPs in Italy. The average concentrations in the influents and effluents were 0.209 μg/L and 0.193 μg/L for carbamazepine, 0.286 μg/L and 0.182 μg/L for sulfamethoxazole, 0.080 μg/L and 0.037 μg/L for trimethoprim. Tisler and Zwiener (2018) investigated the concentrations of metformin in two German WWTPs were in the range of 14 to 95 μg/L for influent and 0.7 to 6.5 μg/L for effluent.

Due to various characteristics of numerous OMPs, there is no specific treatment method that can remove all species of contaminants completely (Luo et al., 2014). In order to improve the water quality and avoid the potential threats of OMPs, reliable and innovative treatment technologies for OMP removal need to be developed and upgraded in WWTPs. The current available technologies include membrane separation processes, ozonation and advanced oxidation processes (AOPs) and adsorption by activated carbon.

1) Membrane separation processes

Membrane separation processes selectively separate micropollutants from the water phase by pore size limitation and by the driving force. The performance of membranes is related to several mechanisms, such as size rejection, electrostatic repulsion, adsorption as well as fouling (Silva et al., 2017). Simon et al. (2009) studied the adsorption of carbamazepine and by NF and RO membranes. High rejection of negatively charged pollutants could be achieved by the electrostatic repulsion mechanism, like sulfamethoxazole at the pH above the pKa. Carbamazepine with a neutral charge in the pH range has no significant variation in membranes separation. De Cazes et al. (2014) reported that membrane bioreactors (MBRs) were more efficient than single membrane or bioprocesses. The performance of MBRs could be optimized by varying operational parameters, such as temperature, pH, fluid velocity, pressure, and HRTs. According to Ma et al. (2018), hydrophobic, nonionized micropollutants showed higher efficiency in sorption in membrane bioreactors, and the biodegradation of micropollutants happened at long SRTs and HRTs.

The major limitation of membrane separation processes is the concentrate containing a high level of OMPs. Shanmuganathan et al. (2017) suggested a membrane filtration - granular activated carbon (GAC) adsorption hybrid system to deal with OMPs and produced concentrates. Additionally, membranes had extremely low removal efficiency of some micropollutants, like carbamazepine and diclofenac (Chon et al., 2011).

2) Ozonation and AOPs

Many studies reported efficient removal of micropollutants from WW by ozonation and AOPs (Sui et al., 2010; Kommineni et al., 2000; De la Cruz et al., 2012). Their performance depends on several factors, such as characteristics of targeted pollutants, ozone and other chemical dosages, and water matrix effect. Ribeiro et al. (2019) observed that natural organic matters (NOMs) and inorganic anions had inhibitory effects on the removal of micropollutants by AOPs. Lee et al. (2014) demonstrated that the removal efficiency of pharmaceuticals at neutral pH varied with ozone dose and hydroxyl radicals generated by hydrogen peroxide. Nakada et al. (2007) reported that the efficiency of ozonation was enhanced by some special structures with donor electrons in micropollutants.

The main disadvantage of AOPs is the formation of toxic by-products including bromate and halogenated organic oxidation by-products (Ike et al., 2019). Another challenge of ozonation and AOPs is the consumption of high energy. Autin et al. (2013) introduced an alternative to provide appropriate irradiance for use in AOPs by UV-LED.

3) Adsorption by activated carbon

Adsorption by activated carbon is a potential technology to remove micropollutants in secondary effluent of WWTPs (Kovalova et al., 2013; Grover et al., 2011; Yang et al., 2011). Removal efficiency by activated carbon is related to activated carbon dose, contact time, particle size of adsorbent, characteristics of pollutants, and water matrix effect. Kennedy and Summers (2015) investigated that adsorption capacity of targeted pollutants increased with longer empty bed contact time (EBCT) and the background dissolved organic matter (DOM) with lower molecular weight. Meinel et al. (2015) compared the performance of granular and powdered activated carbon. Smaller carbon particle size and longer contact time led to better OMP removal. Nguyen et al. (2013) observed that neutral compounds, like carbamazepine, showed slower breakthroughs than negatively charged compounds.

A thermal or chemical regeneration method of GAC could remove adsorbed components. Furthermore, frequent regeneration will increase operating costs.

1.2. OMP adsorption by zeolites

Zeolite adsorption is an alternative technology to remove OMPs in the liquid phase. Zeolites are crystalline aluminosilicates with pores of molecular dimensions that can be entered by molecules (Montalvo et al., 2020). The Structure Commission of the International Zeolite Association gives the framework type of different zeolites. Four commercial types of zeolites are available for academic research and their frameworks are shown in 1.1.

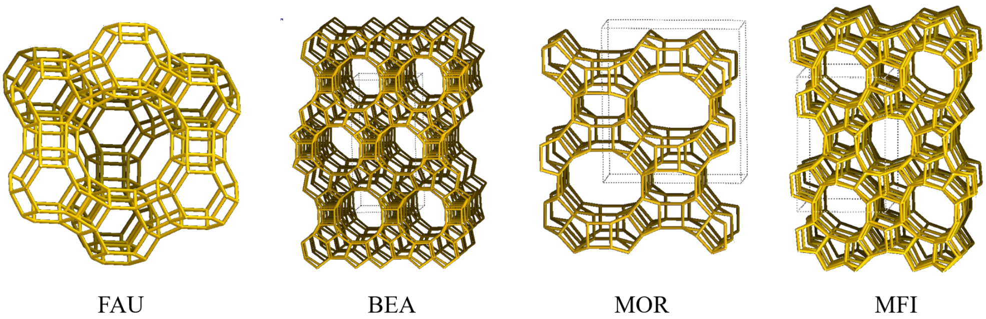

Figure 1.1: Framework type of four zeolites

The performance of zeolites with different frameworks was studied. Khalid et al. (2004) compared the adsorption by HFAU, HMOR, MFI, HBEA and BEA. It was indicated that a zeolitic adsorbent has a hydrophobic property of the molecular sieves for adsorption. BEA could be promising adsorbents with large pores. Jiang et al. (2020) studied the adsorption of triclosan, trichlorophenol and phenol by different zeolite powder, including FAU, BEA, MOR and MFI. The maximum adsorption capacity is related to the micropore volume or micropore surface area of zeolites. Hu (2020) investigated the removal of OMPs by BEA and MOR zeolite granules and found that BEA had better performance than MOR in packed columns.

Various researches studied the adsorption mechanisms of OMPs and the factors affecting the adsorption. Firstly, the structure and micropore size determine the adsorption efficiency of absorbates with different molecular sizes (Li et al., 2005). OMPs with molecular size similar to pore size in zeolites are better removed, and that creates the ”Close-fit” phenomenon (Jiang et al., 2018). The pore volume of the four zeolites mentioned before follows the order of MFI < MOR < BEA < FAU.

Secondly, the surface hydrophobicity of zeolite depends on its silica/alumina ratio. For example, an all-silica BEA zeolite with a meager amount of silanol groups has a high hydrophobicity, which indicates that BEA zeolite is much more hydrophobic than other comparable 12-ring zeolites, such as FAU and MOR (Stelzer et al., 1998; Khalid et al., 2004).

Thirdly, the characteristics of OMPs also affect. There are negatively charged sites on the surface of zeolites, and electrostatic attraction makes stronger adsorption of positively charged OMPs Jiang et al. (2013).

Fourthly, the possible adsorption sites can promote the adsorption of certain OMPs by zeolites. Oxygen and acidic sites are defined as two specific adsorption sites in zeolites. Certain OMPs can be attracted by the hydrogen bonding between zeolite oxygen and the hydrogens of the functional group. The OMPs with acidic hydrogen, like phenolic compounds, can be better adsorbed by zeolites (Koubaissy et al., 2011).

1.3. Modelling in adsorption

The performance of adsorption by absorbent could be compared and quantified by model fitting. Adsorption isotherm models indicate the adsorption capacity of the adsorbent and the adsorption affinity between absorbent and adsorbate. Adsorption kinetics models show the uptake rate of adsorption with respect to time. Breakthrough curves illustrate the dynamic concentration of the effluent through a fixed bed adsorber. The modelling of breakthrough curves could provide helpful suggestions for the design of adsorption treatment process.

1) Adsorption isotherm models

Foo and Hameed (2010) gave a summary of adsorption isotherm models. Langmuir is a well-known model assuming monolayer and homogeneous adsorption, while Freundlich model represents multilayer adsorption in the heterogeneous surfaces. Temperature-dependent Dubinin–Radushkevich model describes a suitable fit at a high and intermediate range of concentrations. Redlich–Peterson model is a hybrid isotherm with the characteristics of Langmuir and Freundlich isotherms and can be applied to heterogeneous or homogeneous systems.

2) Adsorption kinetics models

Pseudo-first-order (PFO) and pseudo-second-order (PSO) models are widely used in adsorption research. Sircar and Hufton (2000) indicated that the PFO model for adsorption kinetics is successfully used to analyze column data, rather than the Fickian Diffusion (FD) model and Quadratic Driving Force (QDF) model. Rodrigues and Silva (2016) carried out that the PFO model is simple but has inconsistent trends theoretically. According to Revellame et al. (2020), the PSO model usually shows higher R^2 than the PFO model due to data processing, while it did not mean the PSO model is the correct one. Intra-particle diffusion (IPD) equation is commonly used to describe kinetics in diffusion-controlled processes while ignore the effect of adsorption (Simonin and Bouté, 2016). The Elovich equation is a commonly used equation to analyze sorption and desorption processes in soil kinetics (Inyang et al., 2016).

3) Prediction of breakthrough curves in the packed column

Xu et al. (2013) elaborated a variety of existing models and theories involved in the modelling of column adsorption systems, such as general rate models, LDF models, wave propagation theory, and Bohart-Adams model. Thomas model is an alternative to predict the breakthrough curve for the effluent in column sorption process (Mathialagan and Viraraghavan, 2002; Uddin et al., 2009). Kalavathy et al. (2010) observed an excellent prediction of metal ion breakthrough curves in columns based on Adam–Boharts model. Azzaz et al. (2017) applied Thomas, dose–response, and Clark models in the prediction of methylene blue breakthrough curves in packed column and showed good results.Heijman et al. (2002) provided a model conception based on mass balance, LDF model and Freundlich model. Aguilera and Ortiz (2016) implemented a one-dimensional mass transfer model by Comsol Multiphysics software and obtained well-matched simulated breakthrough curves of H_2S in the fixed bed.

1.4. Knowledge gaps and research objectives

Critical knowledge gap remained regarding the adsorption of OMPs by zeolite granules in WWTP effluent.

1) Based on the literature review, the adsorption of OMPs in DW by zeolite powder has been well studied previously. There is a need to investigate the performance of zeolite granules for treating OMPs in WW with respect to adsorption capacity and adsorption kinetics.

2) WW contains a variety of background matrices, including NOMs and inorganic ions. The effect of background matrices on OMP adsorption will be investigated by comparing OMP adsorption in DW and in WW.

3) Little is known about the adsorption of OMPs in WW in columns packed by zeolite granules.

4) The link between the adsorption behavior of OMPs in the batch and in the column should be further elaborated in order to understand the adsorption mechanisms of OMPs in zeolite packed column.

Therefore, the objectives of the thesis are:

1) To investigate the adsorption of OMPs in WWTP effluent by zeolite granules in batch and column scales.

2) To clarify the impact of NOMs and ions on the adsorption of OMPs in WWTP effluent.

3) To predict OMP removal in WWTP effluent in columns by a mathematic model.

1.5. Problem statement and research approaches

According to the research objectives, the following research questions were proposed:

1) How does the WW matrix in WWTP effluent influence the adsorption of OMPs by zeolite granules in batch and column experiments?

2) How do NOMs and ions influence the adsorption of OMPs by zeolite granules?

3) How do operational parameters, e.g., different superficial velocities and bed depths, influence the breakthrough curves in columns?

4) What is the performance of the model to predict the breakthrough curves?

In this thesis, the adsorption capacity and kinetics of zeolite granules in the batch require systematic analysis. The breakthrough of OMPs in column scaled experiments will be studied to suggest the column design in practice. Furthermore, a mathematic model applying the parameters of adsorption kinetics and adsorption capacity of OMPs by zeolite granules from batch experiments will be optimized to estimate the breakthrough of OMPs in the effluent of WWTPs by the column packed with zeolite granules. The prediction of breakthrough curves could provide valuable suggestions for column design and optimization of operating parameters.

The schematic research approaches are shown in Figure 1.2.

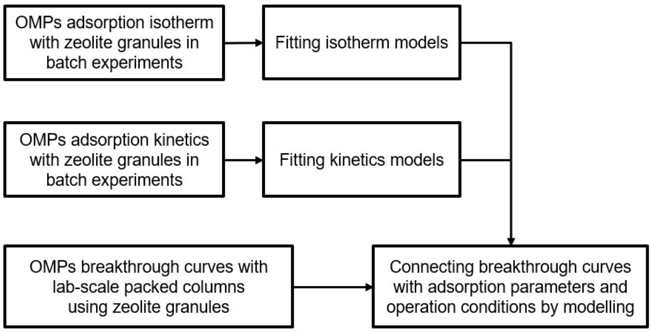

Figure 1.2: Research approaches

2

Materials and methods

2.1. Materials

2.1.1. Zeolite granules

Zeolite granules applied in the research were made of BEA high-silica zeolite powder (Zeolite HSZ-980HOA, Tosoh Corporation, Japan) and bentonite (Sigma-Aldrich, Germany) as the binder. The properties of BEA powder are shown in Table 2.1.

Table 2.1: Properties of BEA zeolite powder

Series	Product name	SiO_2/Al_2O_3 ratio	Surface area (BET, m^2/g)	Cation	Pore size (Å)	Crystal size (μm)	Particle size (μm)
HSZ-900	980HOA	500	500	H^+	6.5	0.5-1	~2.5

*Zeolite properties were obtained from Tosoh Corporation.

Rice-shaped zeolite granules were produced by the 3D printer (LUTUM®) with a zeolite/bentonite weight ratio of 85/15. The printed granules were sintered under 950°C for 2 hours. BEA zeolite granules are shown in figure 2.1. One zeolite granule is approximately $1 \times 1 \times 3$ mm with the weight of 4 ± 0.2 mg. The density of the zeolite granules is about 1.07 g/ml. Zeolite granules were degassed with a vacuum pump in the water matrix for at least 10 minutes before batch and column experiments.

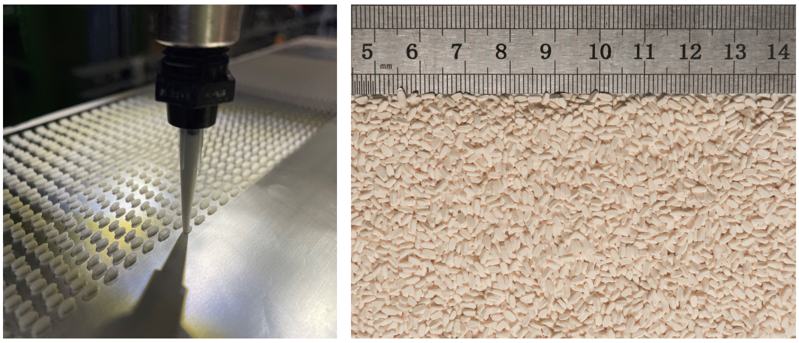

(a)

(b)

Figure 2.1: BEA zeolite granules (a) BEA zeolite granules shaped by 3D-printer ($LUTUM$®)
(b) BEA zeolite granules after sintering

2.1.2. Organic micro-pollutants (OMPs)

A total of 18 target OMPs were selected for studies, which are benzotriazole, methyl-benzotriazole, carbamazepine, diclofenac, hydrochlorothiazide, metoprolol, sulfamethoxazole, propranolol, sotalol, trimethoprim, clarithromycin, ketoprofen, clofibric acid, sulfadimethoxine, caffeine, theophylline, gabapentin, and metformin. The stock solution was prepared by OMP standards (Sigma-Aldrich, Germany). The physiochemical property of the 18 OMPs were shown in Appendix A. The OMP stock solution A (containing benzotriazole, methyl-benzotriazole, carbamazepine, diclofenac, hydrochlorothiazide, metoprolol, sulfamethoxazole, propranolol, sotalol, trimethoprim, and clarithromycin) was prepared by dosing ~2 mg of each OMP standard in 2 L ultrapure water to obtain the concentration of approximately 1 mg/L. In particular, the dosage of methyl-benzotriazole is a mixture of ∼1 mg 4-methyl-1H-benzotriazole and ∼1 mg 5-methyl-1H-benzotriazole. 4- and 5-methyl-1H-benzotriazole are both identified as methyl-benzotriazole in the quantitative analysis. The OMP stock solution B (containing ketoprofen, clofibric acid, sulfadimethoxine, caffeine, theophylline, gabapentin, and metformin) was prepared by dosing ~4 mg of each OMP standard in 1 L ultrapure water to obtain the concentration of approximately 4 mg/L. The stock solutions were kept in the fridge under 4°C.

2.1.3. Water

Demineralised water (DW) and wastewater (WW) were used to prepare water solutions. The WW was the secondary effluent from Horstermeer WWTP. The collected WW was filtered through 1 μm polypropylene cartridge filter (Type PFR01S1AAE, Technofliter, Netherlands) with 99.98% efficiency to remove particles and microorganisms. The filtered WW was stored in the fridge under 4°C before use. The characteristics of WW (Table 2.2) were analyzed after the collection, including pH, UV transmittance (UVT), electrical conductivity (EC), dissolved organic carbon (DOC), cations (i.e., sodium, potassium, calcium and magnesium), and anions (i.e., chloride, nitrite, and sulphate).

Table 2.2: Characteristics of WW

Parameter	unit	value
pH	-	7.76
UVT%	-	60.0±5.4
EC	μS/cm	495
DOC	mg/L	8.3±1.7
Na^+	mg/L	58.6±23.0
K^+	mg/L	17.5±7.9
Ca^{2+}	mg/L	43.9±12.7
Mg^{2+}	mg/L	5.1±1.7
Cl^-	mg/L	80.5±28.2
NO_3^-	mg/L	16.0±5.6
SO_4^{2-}	mg/L	31.1±12.2

2.2. Experimental methods

2.2.1. Batch experiments for adsorption capacity and kinetics

The first series of batch experiments studied the adsorption capacity of 18 OMPs by BEA zeolite granules in DW and WW. The stock solutions A and B were spiked in DW and WW to prepare water solutions with ~8 µg/L OMP each. Different weight of zeolite granules (0, 10, 25, 50, 100, 250, 500, 1000 mg) were dosed in 1 L water solution in Duran glass bottles. The bottles with 0 mg/L zeolite dosage were performed as the blank control group. The glass bottles were placed in an orbital shaker at 120 rpm to reach the equilibrium at 20 ± 1°C. The solution was sampled on day 50. All water samples were analyzed by liquid chromatography–mass spectrometry (LC–MS) to determine OMP concentration.

The second series of batch experiments studied the adsorption kinetics of 18 OMPs BEA zeolite granules in DW and WW. The water solution containing ~4 µg/L OMP each was prepared by spiking the stock solution A and B in DW and WW. The dosages of BEA zeolite granules were 0, 50, 250 and 500 mg/L. The bottles without zeolite dosage were performed as the blank control group to investigate the biodegradation of OMPs. Zeolite dosages of 50 mg/L were conducted in 1L Duran glass bottles, while zeolite dosages of 250 mg/L and 500 mg/L were studied in 250 mL Duran glass bottles. The glass bottles were placed in an orbital shaker being vibrated at 120 rpm at 20 ± 1°C. The solution was sampled at the time interval of 1-42d. The OMP concentration of all water samples was analyzed with LC-MS. The water samples from the WW group were analyzed to quantify DOC, UV-254 and ions.

2.2.2. Column experiments for breakthrough curves

The column experiments were designed to obtain the breakthrough curves of 18 OMPs with BEA zeolite granules. The zeolite granules were packed in the column with the fixed bed depth. The concentrations of OMPs in feed DW and WW were approximately 4 µg/L, which were diluted from the stock solution A and B. To avoid the biodegradation of OMPs, the feed WW stored in 10 L Duran glass bottles was renewed every 2-3 days. A peristaltic pump was used to deliver the flow through the column from top to bottom. The outflow was sampled every 3 h for 14 d by the auto-sampler (BSZ-100, HUXI). All samples were analyzed by LC-MS to obtain the concentration of 18 OMPs after filtration. In addition, DOC, UV-254 and ion concentrations in WW samples were analyzed.

Different experimental conditions were summarized in Table 2.3. Zeolite granules were packed in the glass column with a total length of 40 cm and an inner diameter of 1.89 cm. In the column experiments in DW, the packed bed is 10 cm depth. Two superficial velocities of 0.67 cm/min and 1.67 cm/min were set in columns to simulate different EBCT of 15 min and 6 min. In the column experiments in WW, the breakthrough curves with two bed depths, i.e., 10 cm or 20 cm, were studied. Figure 2.2 shows the experimental set-up of 20 cm depth in WW.

Table 2.3: Experimental conditions of column experiments

No.	Solution	EBCT (min)	Bed depth (cm)	Superficial velocity (cm/min)	Flow rate (ml/min)	Packed weight (g)
1	DW	6	10	1.67	4.68	16.02
2	DW	15	10	0.67	1.87	16.02
3	WW	6	10	1.67	4.68	16.02
4	WW	15	10	0.67	1.87	16.02
5	WW	12	20	1.67	4.68	32.04
6	WW	30	20	0.67	1.87	32.04

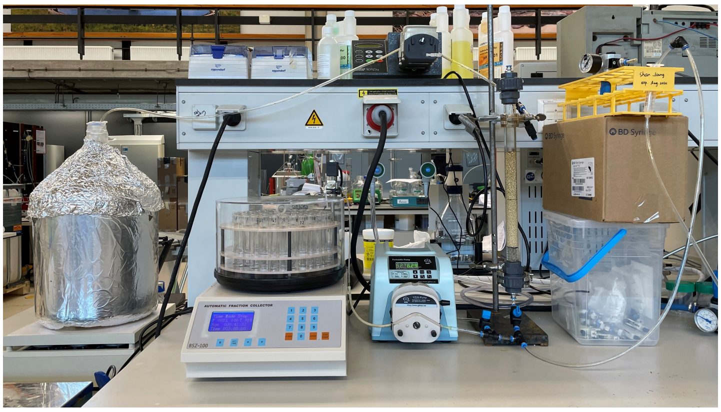

Figure 2.2: Column experimental set-up

2.2.3. Sampling methods

Before LC-MS analysis, water samples were filtered by 0.2 μm membrane filters (Whatman Spartan HPLC certified syringe filters) to remove particles. Since some OMPs in DW were adsorbed by the filter during the filtration, which affects the accuracy of the measurements (Hu, 2020), the sampling and filtration method was modified.

In the experiments in DW, two modified sampling methods were applied:

1) Rinsing the filter with 5 mL tap water and followed by 15 mL water sample. Approximate 1 mL filtrated sample was collected for LC-MS analysis. DOC in tap water will preload the filter and reduce the adsorption of targeted OMPs.

2) Internal standard was spiked in water samples. In this case, 10 µL internal standard was spiked in 990 µL sample and the mixture was filtrated. The filtrated mixture was analyzed by LC-MS. The amount of adsorbed OMPs during filtration was defined by the concentration of internal standard.

As 16 ml water sample was required for filtration, the first method was used in batch experiments in DW. the second method was applied in column experiments in DW, where only 8 ml sample was collected by auto-sampler.

In the experiments in WW, the loss of OMPs during filtration was absent since the filter was loaded by NOMs in WW. Therefore, approximate 5 ml WW samples were filtrated, and ~1 ml filtrated samples were used for LC-MS analysis.

2.2.4. Analysis

LC-MS was used to analyze OMPs. Liquid chromatography separated the sample components through an ACQUITY UPLC®BEH C18 (1.7μm particle size, 2.1×50 mm, Waters, Ireland) column, pumped by an ACQUITY UPLC I-Class Plus System (Waters, USA) at a flow rate of 0.35 ml/min. The gradient elution contained ultrapure water and acetonitrile (LC-MS grade, Biosolve, France) phases, both acidified with 0.1% LC-MS grade formic acid (Biosolve, France). Tandem MS (Xevo TQ-S micro, Waters, USA) separated the ionized molecules by their mass/charge ratio and detected them by corresponding deuterated internal standards. The internal standards (1% vol) were manually added to water samples before analysis. The calibration line, which went from 0.0025 µg/L to 10 µg/L, was prepared by different concentrations of standards. Data were processed through TargetLynx software.

Ion chromatography (IC) was used to quantify ions, which were sodium, potassium, calcium, magnesium, chloride, nitrite, and sulphate in this research. The standard anion column used was A Supp 5 150/4.0, while the standard cation column is C6 Cation 150/4.0. The method for measuring inorganic anions and cations is AnCat Cheryl. For A Supp 5 150/4.0 anion column, the eluent is 3.2 mM Na_2CO_3 and 1 mM $NaHCO_3$ running at 0.7 mL/min. For C6 Cation 150/4.0 anion column, the eluent is 3 mM HNO_3 running at 0.9 mL/min. Water samples were filtrated by 0,2 μm syringe filters

(Whatman Spartan 30/0.20RC Rinse filter) before IC analysis.

UV-254 is the UV absorption spectra of samples measured by UV-Vis spectrophotometer (Genesys 10S) at 254 nm wavelength. Water samples were filtrated by 0,2 μm syringe filters (Whatman Spartan 30/0.20RC Rinse filter) before measurement.

For DOC analysis, water samples were filtrated by 0,45 μm syringe filters (Whatman Spartan 30/0.45RC Rinse filter). Then, 1.6 ml 2M analytical grade hydrochloric acid was added to 30 ml of sample. 10 mg/L total organic carbon (TOC) standard was prepared to check the accuracy of the analyzer. 1.6 ml of 2 M hydrochloric acid was added to 30ml of the standard solution and 30 ml of ultra-pure water, respectively, to prepare standard samples and blank samples. All the samples were finally analyzed by a TOC analyzer.

2.3. Modelling methods

2.3.1. Isotherm models

The adsorption isotherms were fitted by Freundlich model. Freundlich model is an empirical relationship between the concentration of a solute adsorbed onto the surface of a solid and the concentration of the solute in the liquid phase (Equation 2.1), which is applicable for OMP adsorption in zeolite granules. The log-log transformation form of Freundlich model is Equation 2.2.

$$q_e = K_F {C_e}^n \tag{2.1}$$

$$\log q_e = n \log C_e + \log K_F \tag{2.2}$$

where q_e [μg/mg] is the amount of adsorbed solute at equilibrium, C_e [μg/L] is the concentration at equilibrium, K_F [(μg/mg) / (μg/L)^n] is the Freundlich isotherm constant, and n [dimensionless] is the Freundlich intensity parameter.

The linear form (Equation 2.3) is a special case of Freundlich model where the Freundlich intensity parameter n is equal to 1.

$$q_e = K_L C_e \tag{2.3}$$

where K_L [L/mg] is the linear isotherm constant.

2.3.2. Kinetic models

Pseudo – first order (PFO) model describes the adsorption kinetics of a solution onto an adsorbent. The equation is generally written in the natural logarithm form (Equation 2.4). An alternative transformation form (2.5) was used to fit experimental kinetic data.

$$\ln[q_e - q_t] = \ln q_e - kt \tag{2.4}$$

$$q_t = q_e[1 - e^{-kt}] \tag{2.5}$$

where q_e and q_t are the amount of adsorbed solute [μg/mg] at equilibrium and at time t [d], respectively; k [1/d] is the rate constant of the pseudo-first order.

The intra-particle diffusion (IPD) model proposed by Weber and Morris has been widely applied to describe diffusion-controlled processes in liquid/solid adsorption (Equation 2.6).

$$q_t = k_p \sqrt{t} + C \tag{2.6}$$

where k_p [μg / (mg × h$^{1/2}$)] is the rate constant of the IPD model and C [μg/mg] is a constant associated with the thickness of the boundary layer.

2.3.3. Breakthrough curve prediction model

One dimensional mass transfer model was used to predict OMP breakthrough curves in column experiments. The concentration of the OMPs varies with the function of time and position in the column. The differential mass balance for OMPs in the zeolite packed column includes axial dispersion, convective mass transfer, accumulation in liquid phase and adsorption (Equation 2.7).

$$-D_L\frac{\partial^2 C}{\partial z^2}+v\frac{\partial C}{\partial z}+\frac{\partial C}{\partial t}+\frac{(1-\varepsilon)}{\varepsilon}\frac{\partial q_e}{\partial t}=0 \tag{2.7}$$

Where C is the concentration of the OMPs [ug/L], t is the operating time [min], z is the distance from the bed entrance[cm], D_L is the dispersion coefficient [cm^2/min], v is the superficial velocity [cm/min], ρ_b is the bulk density [g/mL], q_e is the adsorption capacity [ug/g], ε is the porosity [-].

The relationship between superficial velocity and flow rate is in Equation 2.8.

$$v=\frac{4Q}{\varepsilon\pi d^2} \tag{2.8}$$

Where Q is the flow rate [cm^3/min], d is the internal diameter of the columns [cm].

In the adsorption process, the mass transfer rate is determined by kinetic constant and the differences between maximum adsorption capacity and specific adsorption capacity (Equation 2.9). The maximum adsorption capacity is obtained by Freundlich equation (Equation 2.10).

$$\frac{\partial q_e}{\partial t}=k(q_e^*-q_e) \tag{2.9}$$

$$q_e^*=K_F C^n \tag{2.10}$$

Where k is the kinetic constant [-], q_e^* represents maximum adsorption capacity at concentration C [ug/g], q_e is adsorption capacity at concentration C at specific time [ug/g], K_F [μg/mg]/(μg/L)^n and n [-] are Freundlich constants.

The initial condition and boundary conditions in the breakthrough curve modeling were set as Equation 2.11, 2.12, 2.13.

Initial condition:

$$C(z,0)=0, q_e(z,0)=0 \text{ for } 0\leqslant z\leqslant L \tag{2.11}$$

Boundary conditions:

$$C(0,t)=C_0 \text{ for } t>0 \tag{2.12}$$

$$\frac{\partial C}{\partial z}(L,t)=0 \text{ for } t>0 \tag{2.13}$$

Where L is total bed depth [m];, C_0 is the OMP initial concentration [μg/L].

The assumptions made to this model include:

- the process is isothermal;
- no chemical reaction occurs in the column;
- the packing material is spherical and uniform in size;
- the bed is homogeneous and the concentration gradient in the radial direction of the bed is negligible;
- the flow rate is constant and invariant with the column position.

By defining the dimensionless variables in Table 2.4, Equation 2.7- 2.13 were converted to Equation 2.14-2.19 for Comsol implementation.

Table 2.4: Dimensionless variables in Comsol implementation

Variables	Expression
Concentration of OMPs in liquid phase	$x = \frac{C}{C_0}$
Concentration of OMPs in solid phase	$y = \frac{q_e}{q^*_{e,0}}$
Distance from the bed entrance	$l = \frac{z}{L}$
Time	$\tau = \frac{t \times v}{L}$
Distribution coefficient	$D_g = \frac{\rho_b \times q^*_{e,0}}{\varepsilon \times C_0}$
Mass transfer coefficient	$S = \frac{k \times L}{v}$
Peclet number	$Pe = \frac{L \times v}{D_L}$

Where $q^*_{e,0}$ is the adsorption loading in equilibrium with the initial concentration [μg/mg].
Mass balance:

$$-\frac{1}{P_e}\frac{\partial^2 x}{\partial l^2} + \frac{\partial x}{\partial l} + \frac{\partial x}{\partial \tau} + D_g \frac{\partial y}{\partial \tau} = 0 \tag{2.14}$$

Adsorption kinetics:

$$\frac{\partial y}{\partial \tau} = S(y^* - y) \tag{2.15}$$

Freundlich isotherm:

$$y^* = \frac{K_F (C_0 x)^n}{q^*_{e,0}} \tag{2.16}$$

Initial condition:

$$x = 0, y = 0 \text{ for } 0 \leqslant x \leqslant L \tag{2.17}$$

Boundary conditions:

$$x(0,\tau) = 1 \text{ for } \tau > 0 \tag{2.18}$$

$$\frac{\partial x}{\partial l}(1,\tau) = 0 \text{ for } t > 0 \tag{2.19}$$

The breakthrough prediction model was implemented in Comsol Multiphysics with the time-dependent and one-dimensional coefficient form partial differential equation (coefficient form PDE) module. The finite element method was used to solve PDE numerically, using the 2-by-1 vector variable $u = \begin{bmatrix} x \\ y \end{bmatrix}$.

The partial differential equation is:

$$e_a \frac{\partial^2 u}{\partial t^2} + d_a \frac{\partial u}{\partial t} + \bigtriangledown \cdot (-c \bigtriangledown u - \alpha u + \gamma) + \beta \cdot \bigtriangledown u + a u = f \tag{2.20}$$

$$\bigtriangledown = \frac{\partial}{\partial x} \tag{2.21}$$

Where the values of the mass coefficient e_a, the damping or mass coefficient d_a, diffusion coefficient c, conservative flux convection coefficient α, conservative flux source γ, convection coefficient β, adsorption coefficient a, source term f are the following:

$$e_a = \begin{bmatrix} 0 & 0 \\ 0 & 0 \end{bmatrix} \qquad d_a = \begin{bmatrix} 1 & D_g \\ 0 & 1 \end{bmatrix} \qquad c = \begin{bmatrix} 1/Pe & 0 \\ 0 & 0 \end{bmatrix} \qquad \alpha = \begin{bmatrix} -1 & 0 \\ 0 & 0 \end{bmatrix}$$

$$\gamma = \begin{bmatrix} 0 \\ 0 \end{bmatrix} \qquad \beta = \begin{bmatrix} 0 & 0 \\ 0 & 0 \end{bmatrix} \qquad a = \begin{bmatrix} 0 & 0 \\ 0 & S \end{bmatrix} \qquad f = \begin{bmatrix} 0 \\ \frac{SK_F(C_0x)^n}{q_0^*} \end{bmatrix}$$

Boundary conditions were defined in Comsol:
Dirichlet boundary type for $l = 0$:

$$r = \begin{bmatrix} 1 \\ 0 \end{bmatrix}$$

Flux-Source type for $l = 0$:

$$-n \cdot (-c \bigtriangledown u - \alpha u + \gamma) = g \cdot qu \tag{2.22}$$

Where the values of boundary flux/source g, boundary adsorption/impedance term q are the following:

$$g = \begin{bmatrix} 0 \\ 0 \end{bmatrix} \qquad q = \begin{bmatrix} 1 & 0 \\ 0 & 0 \end{bmatrix}$$

3

Results and Discussion

3.1. Adsorption capacity

3.1.1. OMP removal in batch experiments

The removal efficiency of 18 OMPs by zeolite granules at zeolite dosage of 1000 mg/L was shown in Table 3.1. According to the removal efficiency by zeolite granules in DW, OMPs were classified into three groups: Good removal with removal efficiency≥90%, Medium removal with removal efficiency 40-90%, and Bad removal with removal efficiency≤40%.

Table 3.1: Removal efficiency of 8 μg/L OMPs with 1000 mg/L zeolite dosage in batch experiments

	OMPs	Charge (pH=7)	Removal efficiency in DW	Removal efficiency in WW
Good removal	Sotalol	+	99.8%	99.7%
	Trimethoprim	+	99.7%	98.5%
	Metformin	+	99.3%	-*
	Propranolol	+	99.1%	100.0%
	Clarithromycin	+	98.5%	50.0%
	Metoprolol	+	98.3%	-*
	Sulfadimethoxine	-	98.2%	97.2%
	Methyl-benzotriazole	-	96.3%	67.6%
	Gabapentin	o	93.6%	-*
	Ketoprofen	-	92.0%	-*
Medium removal	Hydrochlorothiazide	o	79.2%	72.1%
	Benzotriazole	-	74.2%	56.9%
	Caffeine	o	73.9%	-*
	Sulfamethoxazole	-	69.9%	37.9%
	Theophylline	-	54.5%	-*
	Diclofenac	-	40.9%	63.4%
Bad removal	Carbamazepine	o	40.0%	<5.0%
	Clofibric acid	-	34.7%	<10.0%

*biodegraded in WW

It was indicated that positively charged OMPs could be better adsorbed by zeolites than negatively charged and neutral OMPs. The results matched Zheng et al. (2021); Fischer (2020); Ghomashi et al. (2020) observed in earlier studies. A plausible explanation is that the presence of aluminium in zeolites results in a negative charge, which is an ideal trap for cations due to the electrostatic force. The adsorbed cations are relatively movable and could be replaced with positively charged OMPs (Chojnacki et al., 2004; Polat et al., 2004).

Most OMPs had low removal efficiency in WW compared to the experiments in DW. This may be due to the presence of NOMs and ions in the effluent. Hung et al. (2005); Abu-Lail et al. (2010); De Ridder et al. (2012) investigated that natural organic matter (NOMs) does not compete with OMPs in zeolite adsorption because the molecular size of many NOMs is larger than the zeolite channel diameter, and therefore NOMs cannot access the internal pores of zeolites. The presence of background OMPs in the WW matrix might be the reason for the decrease of OMP removal efficiency in the WWTP effluent. The main background OMPs in WWTP effluent are benzotriazole(2.8 μg/L), propranolol(2.0 μg/L), sulfadimethoxine (1.5 μg/L), sotalol (1.2 μg/L), diclofenac (1.0 μg/L), trimethoprim (1.0 μg/L), metformin (1.0 μg/L).

The exception was diclofenac, which showed a high removal efficiency in WW. This might be due to that the ions in the WW matrix improve the adsorption of diclofenac.

Due to the presence of microorganisms in WW, the biodegradation of some species of OMPs happened in batch experiments. After 50 days, the concentrations of metformin, metoprolol, gabapentin, ketoprofen, caffeine and theophylline were close to zero in all groups, including the group without zeolite. For these OMPs, the data could not be used in the removal efficiency calculation and isotherm model fitting.

3.1.2. Effect of zeolite dosage on OMP removal in batch experiments

The effect of zeolite dosage on OMP removal in batch experiments is shown in Figure 3.1, which illustrates that the removal efficiency of OMPs increased with increasing zeolite dosage. The increase can be attributed to the fact that more surface area of zeolite provides more available adsorption sites for interaction with OMPs.

OMPs with good removal achieved a removal efficiency above 80% with a zeolite dosage of 250 mg/L in DW and WW. When the zeolite dosage increased from 250 mg/L to 500 and 1000 mg/L, the removal efficiency increased slowly and reached a plateau. OMPs with medium removal had a nearly linear relationship between the zeolite dosage and removal efficiency.

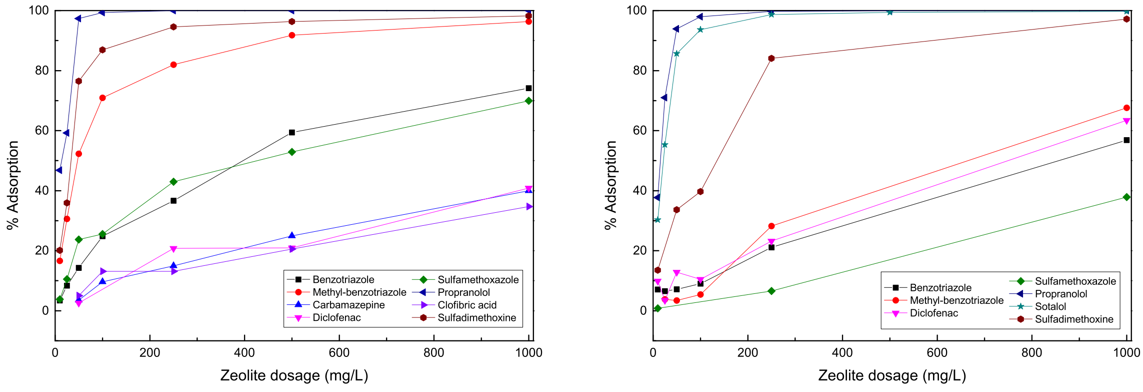

(a) In DW (b) In WW

Figure 3.1: The effect of zeolite dosage on OMP removal
with initial OMP concentration of 8 μg/l and contact time of 50 d

3.1.3. Effect of contact time on OMP removal in batch experiments

The effect of contact time on OMP removal in batch experiments is shown in Figure 3.2. At a zeolite dose of 250 mg/L, the adsorption of different OMPs in DW and WW was nearly completed in 23 d and reached equilibrium. After 23 days, there were rarely available adsorption sites for further OMP adsorption.

After 30 days, a few OMPs came back to the liquid solution from the zeolite, like sulfamethoxazole in DW and benzotriazole in WW. The slight decrease in the removal efficiency might be due to desorption.

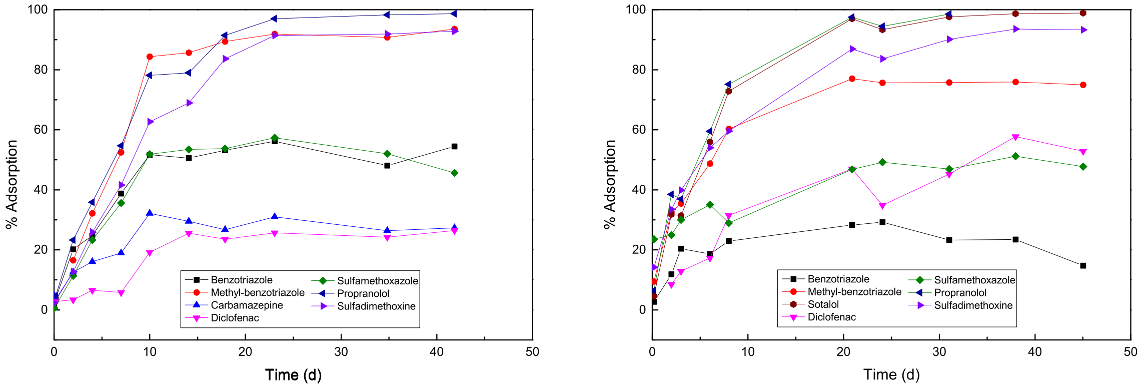

(a) In DW

(b) In WW

Figure 3.2: The effect of contact time on OMP removal
with initial OMP concentration of 4 μg/l and zeolite dose of 250 mg/L

3.1.4. Adsorption isotherms fitting

Freundlich model was utilized to indicate the adsorption capacity of zeolite granules. At the sampling time (50d), OMP adsorption at zeolite dosage of 10 and 25 mg/L did not reach equilibrium yet. Hence, the two sets of points were removed in the data processing. On day 50, the equilibrium concentration of a few well-adsorbed was below the detection limit. Their data were not fitted with isotherm models. Badly removed OMPs with equilibrium concentration close to initial concentration were omitted in Freundlich model fitting. Inaccurate measurement of hydrochlorothiazide and clarithromycin in batch experiments leads to invalid isotherm and kinetic results.

The adsorption capacity of OMPs by zeolite granules was discussed in this section by referring to available Freundlich model fitting results. The comparison of Freundlich and linear models is shown in Appendix B.

Figure 3.3 presents the adsorption isotherms of OMPs by zeolite granules in DW and WW fitted by Freundlich model. With OMPs less than 10 μg/L, the equilibrium adsorption amount of zeolite was 2-100 ug/g in DW and 0.2-101 ug/g in WW for different OMPs at 20°C.

Freundlich fitting constants for OMP adsorption in DW and WW are listed in Table 3.2. The values of affinity coefficient n in Freundlich model are in the range of 0.45-1.95 in DW, and 0.53-1.94 in WW. Values n of most OMPs in WW are smaller than 1, except for trimethoprim and ketoprofen.

When n is smaller than 1, high affinity of the adsorbent zeolite takes place at low concentrations of OMPs. When n is equal to 1, there is a linear relationship between the OMP concentration and its adsorption capacity. When n is larger than 1, a greater affinity is indicated at larger loading of OMPs.

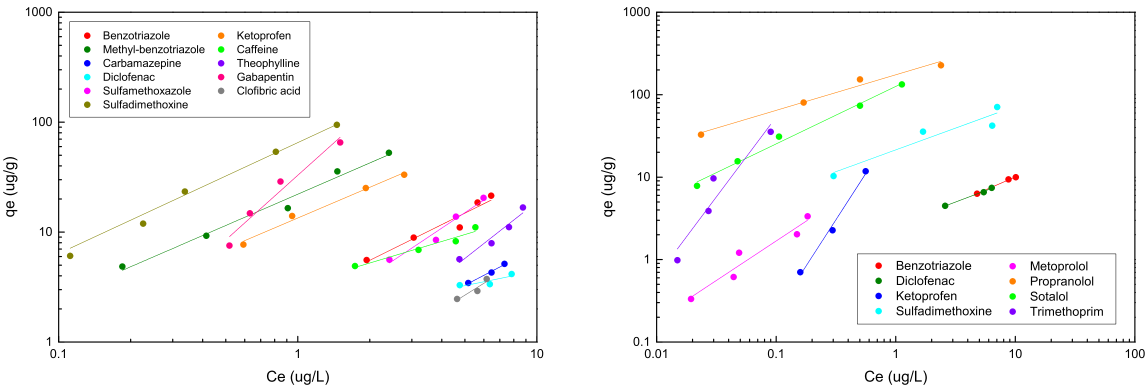

(a) In DW (b) In WW

Figure 3.3: Adsorption isotherms in DW and WW fitted by Freundlich model.

Table 3.2: Freundlich constants for OMP adsorption in DW and WW

	In DW			In WW		
OMPs	K_F	n	R^2	K_F	n	R^2
Benzotriazole	2.6	1.08	0.94	2.4	0.63	0.99
Methyl-benzotriazole	22.1	0.94	0.98	-	-	-[c]
Carbamazepine	0.5	1.13	0.99	-	-	-[d]
Diclofenac	1.6	0.45	0.77	2.7	0.55	0.99
Hydrochlorothiazide	-	-	-[a]	-	-	-[a]
Metoprolol	-	-	-[b]	15.3	0.96	0.92
Sulfamethoxazole	1.5	1.45	0.98	-	-	-[d]
Propranolol	-	-	-[b]	204.0	0.49	0.99
Sotalol	-	-	-[b]	125.9	0.70	0.99
Trimethoprim	-	-	-[b]	4617.0	1.94	0.97
Clarithromycin	-	-	-[a]	-	-	-[a]
Ketoprofen	13.4	0.93	0.99	40.5	2.25	0.99
Clofibric acid	0.3	1.36	0.89	-	-	-[d]
Sulfadimethoxine	66.2	1.08	0.99	21.4	0.53	0.79
Caffeine	3.3	0.65	0.93	-	-	-[c]
Theophylline	0.4	1.71	0.94	-	-	-[c]
Gabapentin	32.9	1.95	0.98	-	-	-[c]
Metformin	-	-	-[b]	-	-	-[c]

[a] Invalid results due to inaccurate measurement
[b] Invalid results due to low concentration below the detection limit
[c] Invalid results due to biodegradation within 50 days
[d] Invalid results due to equilibrium concentration close to initial concentration

3.1.5. Effect of WW matrix on adsorption capacity

Positively charged OMPs were well removed in DW with the equilibrium concentrations below the detection limits. Likewise, batch experiments in WW indicated good removal of these OMPs. The equilibrium concentrations in WW exceeded the detection limits and their isotherm constants were studied. The removal efficiencies of positively charged OMPs in WW were lower than those in DW.

Neutral OMPs, including carbamazepine, gabapentin and caffeine, showed different performance in

DW and WW. Carbamazepine was partly adsorbed in DW with the removal efficiency of approximately 40% but hardly removed in WW. Gabapentin and caffeine were biodegraded in WW and their adsorption performance cannot be studied.

The available adsorption isotherms of four negatively charged OMPs could be compared in DW and WW are diclofenac, ketoprofen, benzotriazole and sulfadimethoxine.

Diclofenac and ketoprofen are negatively charged compounds with a net charge of -1.00 at pH = 7. Compared to isotherms in DW, diclofenac and ketoprofen have bigger K_F and bigger n in WW (Table 3.2), which indicates higher adsorption capacity and better affinity under higher concentration in WW. This might be due to the presence of cations in WW.

Benzotriazole and sulfadimethoxine are negatively charged compounds, with a net charge of -0.02 and -0.55 at pH = 7, respectively. These two compounds have smaller K_F and smaller n in WW (Table 3.2), which indicated the lower adsorption capacity and weaker affinity under higher concentration in WW. This might be due to the presence of background matrices in WW.

WW matrix has different effects on zeolite adsorption isotherm constants of different species of OMPs.

3.2. Adsorption kinetics

3.2.1. Biodegradation in WW

In the kinetic experiment, some OMPs were partly or completely biodegraded by the microorganisms in WW. Figure 3.4 shows the OMP concentration of the blank control group in WW changing with time. The biodegradation of caffeine, theophylline and gabapentin occurred at ~day 8 and completely biodegraded on day 30 (Figure 3.4(a)). Extraordinarily, the concentration of methyl-benzotriazole in blank samples was half of the initial concentration after 13 days, which indicates that one of the compositions (4- or 5-methyl-benzotriazole) was degraded. The biodegradation of metoprolol, trimethoprim, ketoprofen and metformin after 21 days was shown in Figure 3.4(b). The rest OMPs were not biodegraded (Figure 3.4(c)).

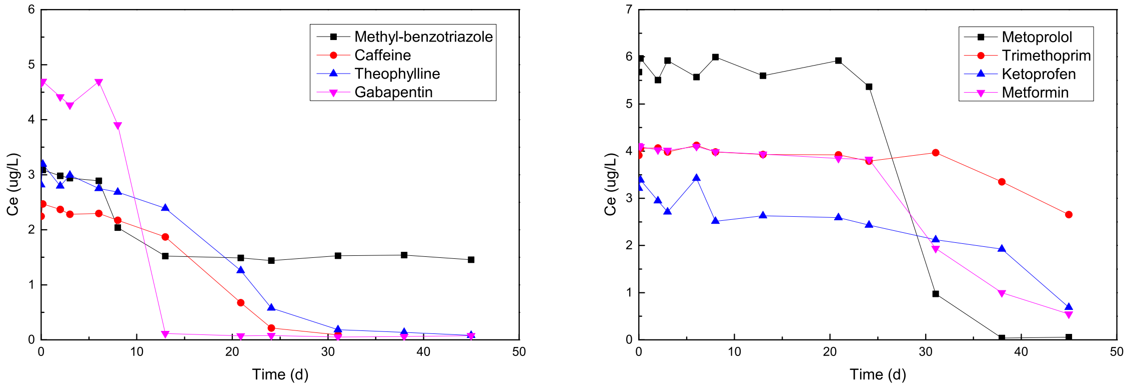

(a) Biodegradation after 8 d

(b) Biodegradation after 21 d

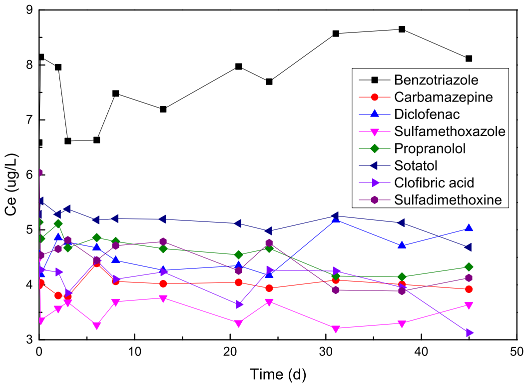

(c) No biodegradation

Figure 3.4: Results of the blank control group in WW batch experiments

3.2.2. Adsorption kinetics fitting methods

In PFO fitting, there were two ways to determine the value of q_e and k. 1) Setting the initial values of q_e and k and finding the best fit. 2) estimating k by the fixed q_e, which was acquired from Freundlich model.

The equation to obtain the value of fixed q_e based on Freundlich model is listed in Equation 3.1.

$$q_e = \frac{1000(C_0 - C_e)V}{W} = K_F {C_e}^n \tag{3.1}$$

where q_e [μg/g] is the equilibrium amount of adsorbed solute in kinetic batches, C_0 [μg/L] is the equilibrium concentration of the blank control group, C_e [μg/L] is the equilibrium concentration of the experimental group, V [L] is the volume of the solution, W [mg/L] is the zeolite dosage, K_F [(μg/mg) / (μg/L)^n] and n are the Freundlich constants obtained in section 3.1. C_e is the only unknown variable in the right two expressions. For OMPs with invalid Freundlich model constants, the linear isotherm constants K_L were used. PFO constants cannot be calculated with Method 2 for the adsorption of caffeine, theophylline, gabapentin and metformin in WW, due to the biodegradation and the absence of isotherm constants.

Figure 3.5 compares the performance of two methods for PFO fitting. Propranolol represents the OMPs with good data quality. The two predicted curves both have a perfect fit and similar values of q_e and k. Sulfamethoxazole represents the OMPs with outliers in kinetic data. When the kinetic curve is smooth, in other words, of good quality, the two methods showed similar results. Otherwise, when the data quality is poor, two fittings are different. In the following part, the first method was applied to fit the adsorption kinetic data.

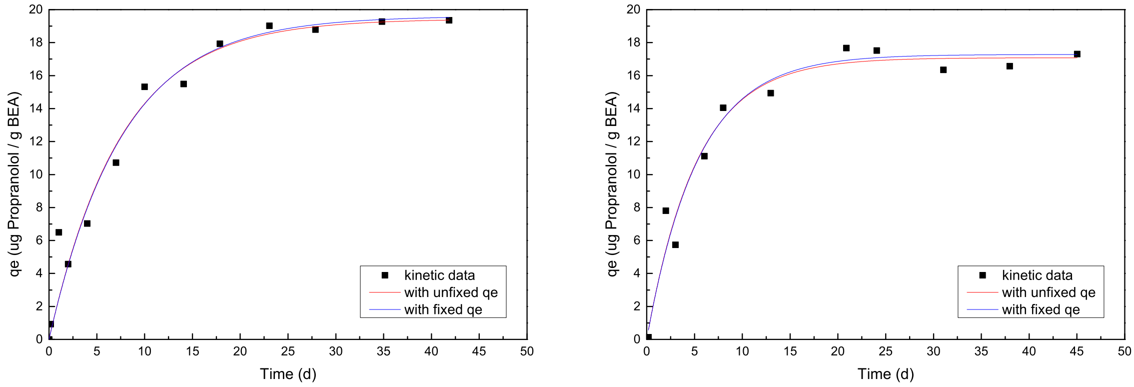

(a) Propranolol in DW (b) Propranolol in WW

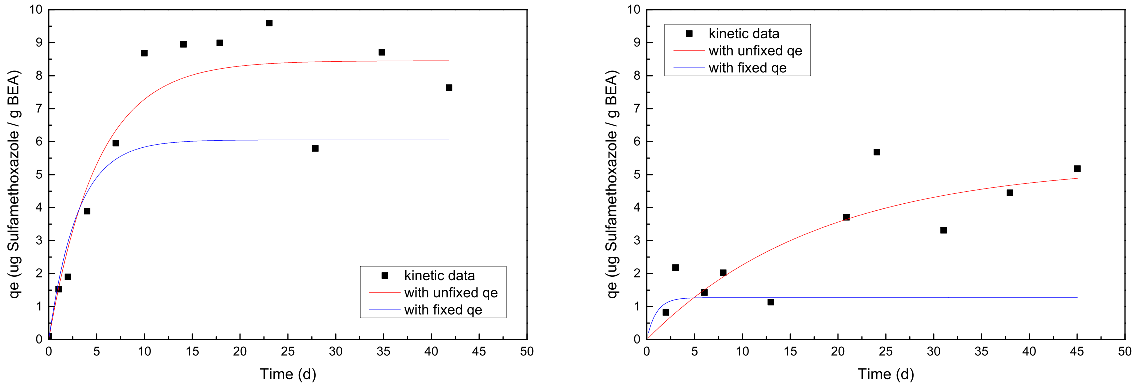

(c) Sulfamethoxazole in DW (d) Sulfamethoxazole in WW

Figure 3.5: Kinetics of propranolol and sulfamethoxazole with zeolite dosage of 250 mg/L in DW and WW

3.2.3. Adsorption kinetics fitting

After the batch experiments for 45 days, the groups with 50 mg/L zeolite dosage did not reach the equilibrium and it is unavailable to get a value of q_e from the experimental data. Experimental data with zeolite dosages of 250 mg/L and 500 mg/L were fitted with the PFO model. Figure 3.6 shows the kinetics of sotalol as the example of PFO fitting in DW and WW. The complete PFO fitting results are plotted in Appendix C.

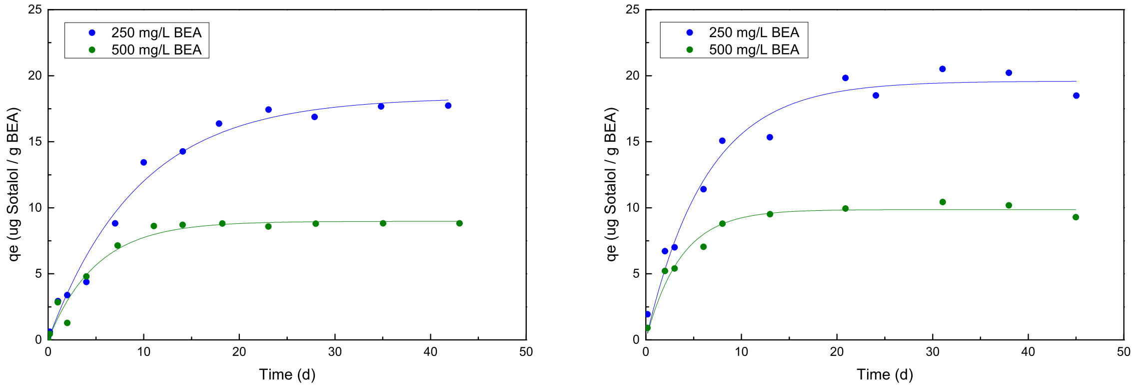

(a) Sotalol in DW

(b) Sotalol in WW

Figure 3.6: The kinetics of sotalol with zeolite dosage of 250 and 500 mg/L in DW and WW

The PFO constants for OMP adsorption in DW and WW with zeolite dosage of 250 mg/L and 500 mg/L are listed in Table 3.3. *k*250 and *k*500 represent the kinetic constants at zeolite dosage of 250 mg/L and 500 mg/L, respectively. The data points below the detection limits were excluded before model fitting.

Table 3.3: Kinetic constants for OMP adsorption in DW and WW with zeolite dosage of 250 mg/L and 500 mg/L

	In DW				In WW			
OMPs	*k*250[1/d]	R^2	*k*500[1/d]	R^2	*k*250[1/d]	R^2	*k*500[1/d]	R^2
Benzotriazole	0.229	0.94	0.180	0.91	-	-	0.168	0.24
Metformin	0.116	0.97	-	-	0.213	0.97	0.331	0.97
Methyl-benzotriazole	0.142	0.97	0.201	0.96	1.274	0.66	1.978	0.73
Gabapentin	0.134	0.94	0.193	0.96	0.156	0.86	0.506	0.84
Theophylline	0.206	0.88	0.151	0.72	-	-	-	-
Caffeine	0.226	0.74	0.139	0.78	0.282	0.53	0.446	0.94
Clofibric acid	-	-	-	-	-	-	-	-
Carbamazepine	0.282	0.88	0.086	0.86	-	-	-	-
Sulfamethoxazole	0.198	0.92	0.165	0.91	0.055	0.73	-	-
Ketoprofen	0.080	0.95	0.091	0.90	0.196	0.72	0.315	0.83
Propranolol	0.133	0.97	0.261	0.96	0.188	0.96	0.309	0.92
Metoprolol	0.153	0.86	0.439	0.94	0.153	0.96	0.270	0.97
Sotalol	0.106	0.99	0.194	0.96	0.159	0.96	0.284	0.96
Trimethoprim	0.111	0.98	0.215	0.98	0.162	0.94	0.272	0.96
Diclofenac	0.094	0.92	0.080	0.65	0.015	0.71	0.094	0.78
Hydrochlorothiazide	0.342	0.59	0.103	0.52	-	-	-	-
Sulfadimethoxine	0.098	0.97	0.152	0.96	0.104	0.94	0.143	0.94
Clarithromycin	-	-	-	-	-	-	0.124	0.96

*OMPs are sorted in ascending order of molecular weight

3.2.4. Effect of zeolite dosage on adsorption kinetics

According to Table 3.3, all the values of $k500$ were greater than $k250$ in WW. By calculation, the ratios of $k500$ to $k250$ in WW were in the range of 1.5-1.8 in most cases. In theory, adsorption kinetic constants increase with an increase in the adsorbent dosage due to the increased adsorption sites. It is consistent with Ho and McKay (1998)'s study for the sorption of basic dyes by sphagnum moss peat and Demirbas et al. (2009)'s study for the adsorption of copper using hazelnut shell activated carbon.

Whereas in DW, half of the $k500$ values were larger than $k250$, and the other half were not. It is possibly caused by data errors. The OMPs showing opposite effects of zeolite dosage on adsorption kinetics usually had less smooth curves shown in Appendix C.

3.2.5. Effect of WW matrix on adsorption kinetics

In accordance with Table 3.3, it is indicated that most OMPs have greater adsorption kinetic constants in WW rather than in DW, including metformin, methyl-benzotriazole, gabapentin, caffeine, propranolol, ketoprofen, sotalol and trimethoprim. Benzotriazole, sulfamethoxazole and metoprolol follow the opposite trend.

Previous studies found that the PFO constants decreased with increasing of the initial adsorbent concentration in most cases (Mansouriieh et al., 2016; Wu et al., 2015; Demirbas et al., 2008). In our case, the group in the WW matrix had a higher OMP concentration which might lead to a decrease in PFO constants with the same amount of adsorbent.

3.2.6. Effect of molecular weight on adsorption kinetics

In Table 3.3, the OMPs are sorted in ascending order of molecular weight. $k500$ in WW followed a decreasing order: gabapentin > caffeine > ketoprofen > propranolol > metoprolol ≈ sotalol ≈ trimethoprim > sulfadimethoxine > clarithromycin, which is consistent with the order of molecular weight. $k250$ in WW followed a similar descending order: caffeine > ketoprofen > propranolol > metoprolol ≈ sotalol ≈ trimethoprim > sulfadimethoxine, which is consistent with the molecular weight order. It is assumed that the large molecular weight of OMPs can be the limitation of kinetic constants. Previous studies (Dijt et al., 1990; Aoki and Adachi, 2006) reported a similar trend in adsorption kinetics of polymer, i.e., a lower mass transfer rate for long-chain polymers. The explanation is that adsorbates with larger molecular weight have lower diffusion constants, which leads to lower mass transfer rates.

3.3. Results of column experiments

3.3.1. OMP removal in zeolite packed column

The removal efficiencies of OMPs in zeolite packed column were represented by the percentage of OMP concentration in the outlet of the column relative to OMP concentration in the column inlet. In accordance with the removal performance of OMPs in column experiment in 14 days, 18 OMPs were categorized into three groups in Table 3.1, namely Good removal, Medium removal, and Bad removal.

Table 3.4: Removal efficiency of 4 μg/L OMPs in zeolite packed columns

	OMPs in DW	OMPs in WW
Good removal	Sotalol Metformin Metoprolol Trimethoprim Gabapentin Methyl-benzotriazole Clarithromycin Propranolol	Sotalol Trimethoprim Metoprolol Propranolol Metformin
Medium removal	Sulfadimethoxine Sulfamethoxazole Ketoprofen Benzotriazole Hydrochlorothiazide Caffeine Theophylline Carbamazepine	Ketoprofen Sulfadimethoxine Methyl-benzotriazole Gabapentin Caffeine Clarithromycin Benzotriazole Sulfamethoxazole Theophylline Diclofenac Clofibric acid Carbamazepine
Bad removal	Diclofenac Clofibric acid	

*Hydrochlorothiazide had inaccurate measurement.

*OMPs in the list were ordered from best removal to worst removal.

The OMP removal in the column was similar to that in the batch. OMPs in the good removal group were well removed in columns over 14 days and shows flat breakthrough curves at low levels. The good removal group includes all positively charged OMPs and a few negatively charged OMPs. The medium removal group represents OMPs with rising breakthrough curves, indicating that these OMPs were well removed initially and the removal efficiency decreased with time. Most neutral or negatively charged OMPs belongs to the medium removal group. Diclofenac and clofibric acid were barely adsorbed in zeolite packed columns in DW and are classified as the bad removal group. Clofibric acid, diclofenac and carbamazepine were consistently the three least effective compounds for removal, whether in batches or columns, in DW or WW.

3.3.2. Breakthrough curves in DW

Figure 3.7 illustrates the breakthrough curves for OMP adsorption in the zeolite packed columns in DW.

The concentration ratios $C/C0$ of OMPs with good removal were below 0.1 over 14 days with no significant increase. The breakthrough curves of methyl-benzotriazole, clarithromycin and gabapentin

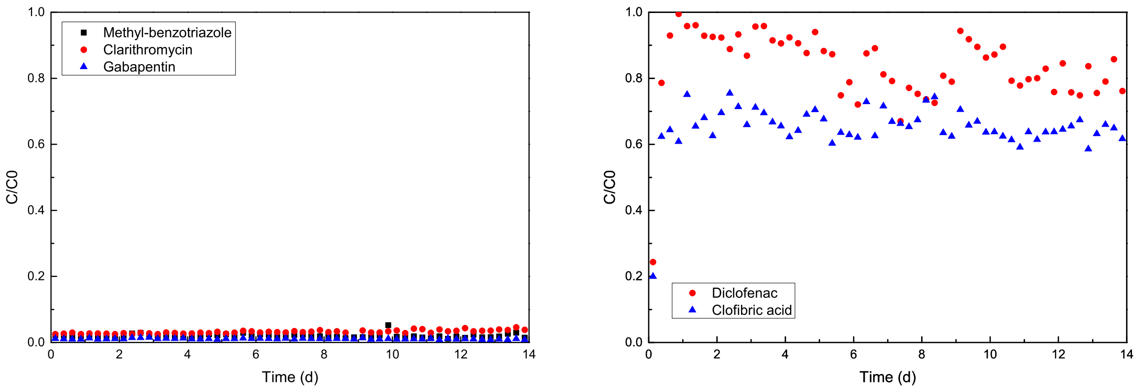

(a) OMPs with good removal (b) OMPs with bad removal

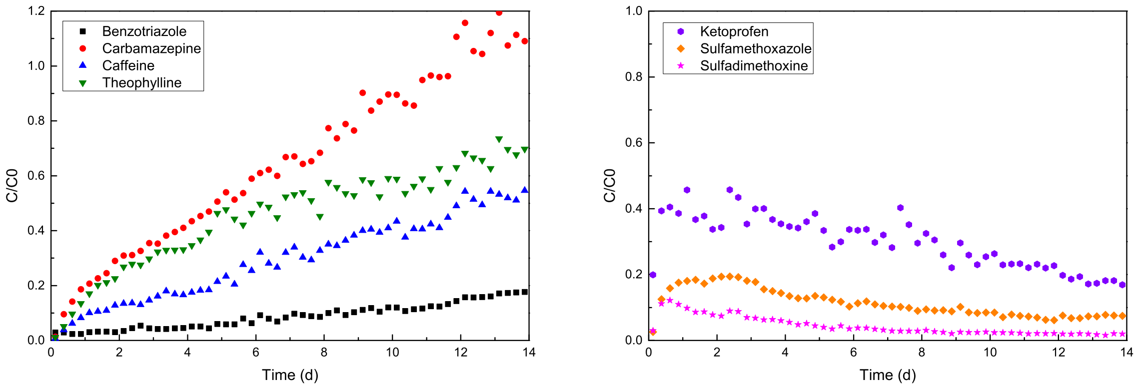

(c) OMPs with medium removal (I) (d) OMPs with medium removal (II)

Figure 3.7: Breakthrough curves for OMP adsorption in zeolite packed columns in DW with EBCT = 15 min, and bed depth = 10 cm

are shown in Figure 3.7(a). A few OMPs had outlet concentrations below the detection limits, which were sotalol, metformin, metoprolol, trimethoprim and propranolol. For OMPs with bad removal, $C/C0$ exceeded 0.6 for clofibric acid and 0.8 for diclofenac (Figure 3.7(b)). OMPs with medium removal usually showed increasing breakthrough curves, such as benzotriazole, carbamazepine, caffeine and theophylline (Figure 3.7(c)). With the EBCT of 15 min, $C/C0$ of carbamazepine, theophylline, and caffeine reached 50% on day 5, 7 and 12, respectively. Benzotriazole had a $C/C0$ of less than 0.2 after 14 days. Ketoprofen, sulfamethoxazole and sulfadimethoxine showed a special case (Figure 3.7(d)). Their removal efficiencies increased at the beginning and then declined. The reason for this may be that, with the adsorption of positively charged OMPs, more cations are freed in the liquid phase with the ion exchange process of zeolite adsorption. The cations improved the adsorption of these three negatively charged OMPs. The special case only occurred in DW.

3.3.3. Breakthrough curves in WW

Figure 3.8 indicates the breakthrough curves for OMP adsorption in the zeolite packed columns in WW.

In the group with good removal, trimethoprim and metformin showed flat breakthrough curves with $C/C0$ of less than 0.1 at 14 days (Figure 3.8(a)). Sotalol, metoprolol and propranolol were well removed with outlet concentrations below the detection limits. Most OMPs were classified to the medium removal group. In Figure 3.8(b), a few OMPs had increasing breakthrough curves and had not plateaued after 14 days of operation. Clarithromycin was the only positively charged OMPs with $C/C0$

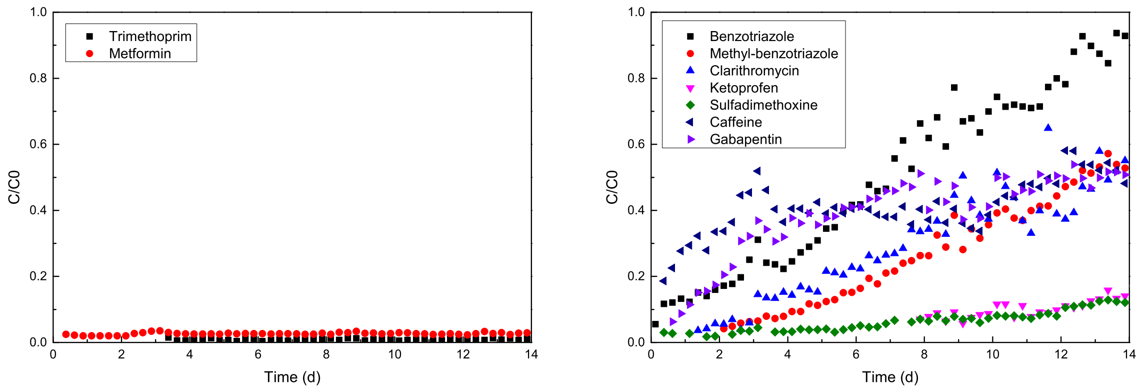

(a) OMPs with good removal (b) OMPs with medium removal (I)

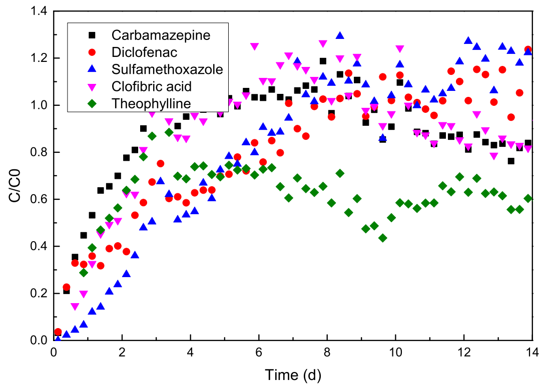

(c) OMPs with medium removal (II)

Figure 3.8: Breakthrough curves for OMP adsorption in zeolite packed columns in WW with EBCT = 15 min, and bed depth = 10 cm

above 0.5 over 14 days. The reason could be that the large molecular size of clarithromycin restricted access to the internal pore of zeolite granules. In Figure 3.8(c), the rest OMPs were poorly adsorbed in the zeolite packed column and reached a plateau within 14 days.

3.3.4. Effect of WW matrix on breakthrough curves

According to the differences between the breakthrough curves in the packed zeolite columns in DW and WW, OMPs were divided into four categories. Figure 3.9 represents the adsorption behaviour of Type II, Type III and Type IV.

- Type I: sotalol, metformin, trimethoprim, metoprolol, propranolol, ketoprofen, and sulfadimethoxine

The first type is the OMPs with high removal efficiencies of over 90% and flat breakthrough curves both in DW and WW. WW matrix had small influence on these OMPs, only slightly decreased their removal efficiencies. Most positively charged OMPs were classified to Type I.

- Type II: benzotriazole, sulfamethoxazole, methyl-benzotriazole, clarithromycin, caffeine and gabapentin

Benzotriazole (Figure 3.9(a)) and sulfamethoxazole (Figure 3.9(b)) represent the adsorption behaviour of Type II. These OMPs were well adsorbed in DW with removal efficiencies of over 90% during 14

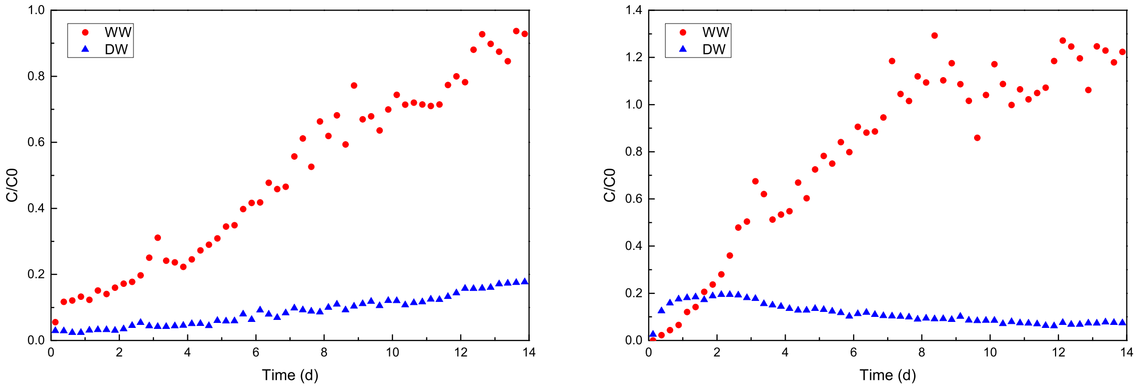

(a) Benzotriazole (b) Sulfamethoxazole

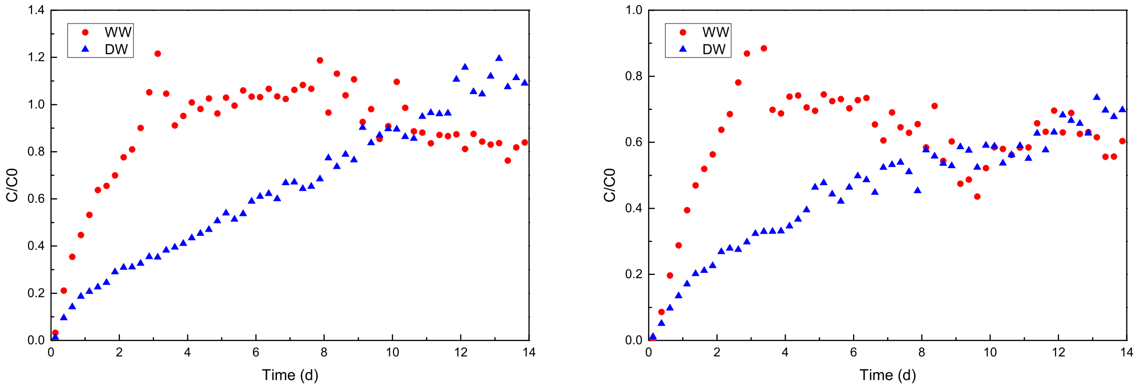

(c) Carbamazepine (d) Theophylline

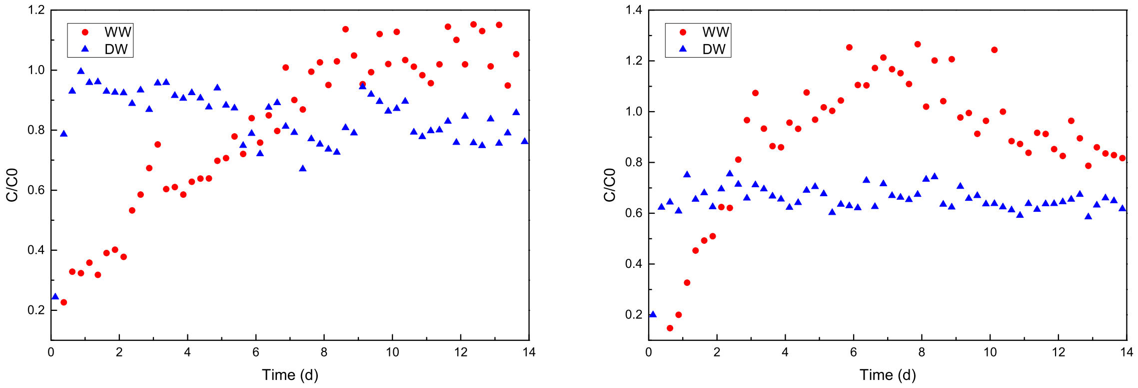

(e) Diclofenac (f) Clofibric acid

Figure 3.9: The effect of WW matrix on breakthrough curves in the columns with EBCT = 15 min, and bed depth = 10 cm

days. Their breakthrough curves were at low levels. In WW, the breakthrough curves showed an increasing trend. The concentration ratio of benzotriazole in outlet to that in inlet increase from ~0% to ~95% in 14 days. For sulfamethoxazole, the column was saturated after 8 days.

In the WW matrix, these OMPs had a much earlier breakthrough, even achieved the plateaus.

- Type III: carbamazepine and theophylline

Carbamazepine (Figure 3.9(c)) and theophylline (Figure 3.9(d)) had increasing breakthrough curves in DW and almost reached the plateaus over 14 days. Their removal was effective in DW for the first ~10 days. In WW, these OMPs were saturated in an early time, about three days. After that, the concentration ratios kept at a high level. Type II can be regarded as the early stage of Type III.

The WW matrix decreased the removal of these two OMPs and shortened the saturation time. Using the WW matrix with the EBCT of 15 min, it was not possible to achieve the required removal.

- Type IV: diclofenac and clofibric acid

Diclofenac (Figure 3.9(e)) and clofibric acid (Figure 3.9(f)) showed flat breakthrough curves with low removal efficiencies during the column experiment in DW. These two compounds were weakly adsorbed by zeolite packed column in DW. Diclofenac and clofibric acid could be adsorbed in WW matrix, with initial removal efficiencies of over 80%. Their removal efficiencies decreased with time and showed increasing breakthrough curves. It is hypothesised that the cations in WW contributed to the adsorption of these two compounds.

WW matrix altered the adsorption behaviour of diclofenac and clofibric acid and made them easier to remove.

In summary, WW matrix had little effect on most positively charged compounds, while the removal of most negatively charged compounds was reduced. Consistent with the results of batch experiments, it might be that the background matrices in WW would decrease the removal efficiencies of target OMPs. In addition, WW matrix could contribute to the adsorption of a few negatively charged compounds, such as diclofenac and clofibric acid, which is possibly due to the presence of cations.

3.3.5. Effect of operational parameters on breakthrough curves

The OMP removal in the zeolite packed columns with different combinations of EBCTs and bed depths was studied. To investigate the effect of operational parameters on breakthrough curves in columns, the breakthrough curves were prepared for the variation of $C/C0$ as a function of cumulative effluent volume. Cumulative effluent volumes can be calculated by Equation 3.2.

$$V = Q \cdot t \tag{3.2}$$

where V [L] is the cumulative effluent volume, Q [L/d] is the flow rate, t [d] is the operation time.

The effect of velocity on the breakthrough curves for OMP adsorption was studied in Figure 3.10 by examining two velocities of 1.67 and 0.67 cm/min through zeolite packed columns with the same bed depth of 20 cm. The results showed that the column would be saturated at a similar operation time at different velocities, e.g., $C/C0$ for sulfamethoxazole reached ~0.8 on day 35 at the two different velocities. Before the saturation, comparisons of the removal of sulfamethoxazole, caffeine, theophylline and gabapentin in zeolite packed column showed that the higher performance was formed at a slower velocity. The reason can be that a larger velocity could attribute to the insufficient residence time of OMPs in columns, which limits the diffusion of OMPs for getting into the internal pores of zeolites. The finding is consistent with the study from Dolatyari et al. (2017).

The effect of bed depth on the breakthrough curves for OMP adsorption in zeolite packed columns was investigated in Figure 3.11 by conducting two bed depths of 10 and 20 cm at the same velocity of 1.67 cm/min. The breakthrough curves of sulfamethoxazole indicated that the columns at different bed depths would have a similar saturation time. Before reaching saturation, more extended bed depths led to better adsorption of OMP in the zeolite packed columns. This can be explained by the increased surface area of the zeolite adsorbent and more contact time. According to the previous studies (Dolatyari et al., 2017; Chatterjee and Schiewer, 2011), the greater the bed depth, the wider the mass transfer zone. The dispersion of OMPs in the columns increased with length, making it more difficult to saturate the column thoroughly. Thus, the slope of the breakthrough curve decreased with a larger bed depth.

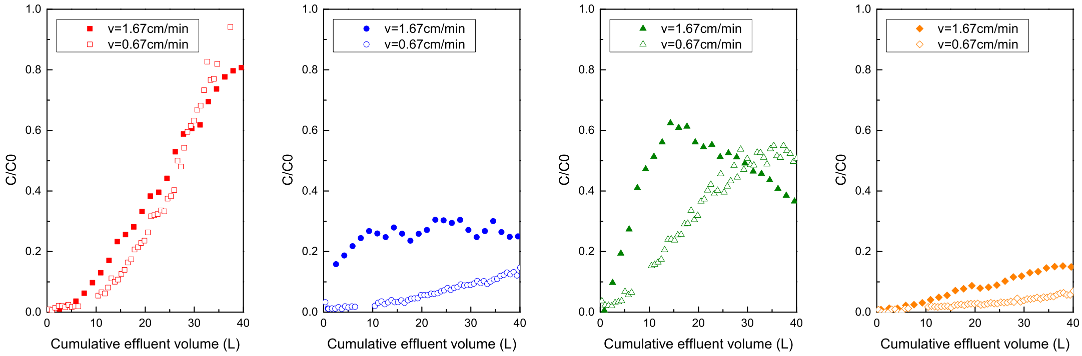

(a) Sulfamethoxazole (b) Caffeine (c) Theophylline (d) Gabapentin

Figure 3.10: Breakthrough curves for OMP adsorption in zeolite packed columns in WW at different velocities and fixed bed depth of 20 cm

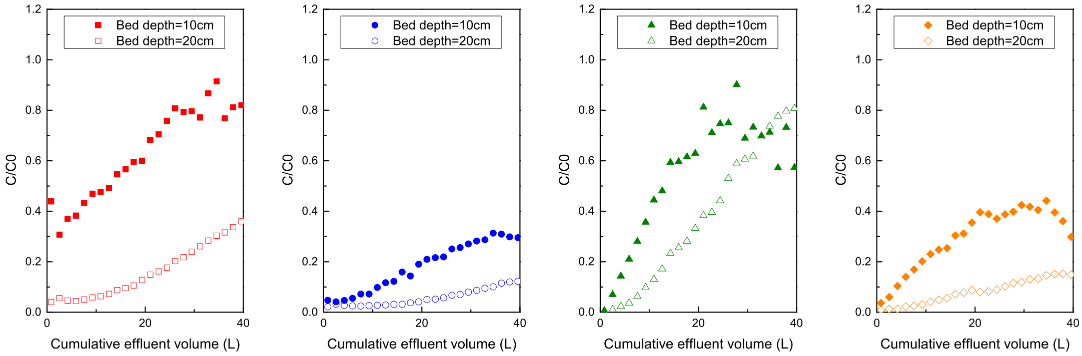

(a) Benzotriazole (b) Methyl-benzotriazole (c) Sulfamethoxazole (d) Gabapentin

Figure 3.11: Breakthrough curves for OMP adsorption in zeolite packed columns in WW at different bed depths and fixed velocity of 1.67 cm/min

As EBCT depends on velocity and bed depth, it could be concluded that a longer EBCT could promote the performance of the zeolite packed column and provide a better removal before saturation. A long contact time provides sufficient time for the OMPs to diffuse and enter the internal pores of the zeolite.

3.3.6. Evaluation of the adsorption by zeolite packed columns with different operational parameters

One of the targets of this study was to provide suggestions for the design of parameters for OMP adsorption in zeolite packed column systems in WW. It was assumed that a removal efficiency above 50% could be regarded as effective. The variation of $C/C0$ as a function of time for the adsorption of OMPs onto the zeolite columns was plotted to compare the column performance at different of EBCTs and bed depths.

A few OMPs were well removed in WW at different of EBCTs (6, 12, 15 and 30 min) with the removal efficiency above 80% over 14 days, i.e., sotalol, trimethoprim, metoprolol, propranolol, metformin, ketoprofen and sulfadimethoxine.

Figure 3.12 showed that these five OMPs were effectively removed in the columns at the EBCT of 12 and 15 min. For benzotriazole, $C/C0$ reached 50% at day ~8. Methyl-benzotriazole, clarithromycin, gabapentin and caffeine reached the requirement with $C/C0$ less than 50% before day 12.

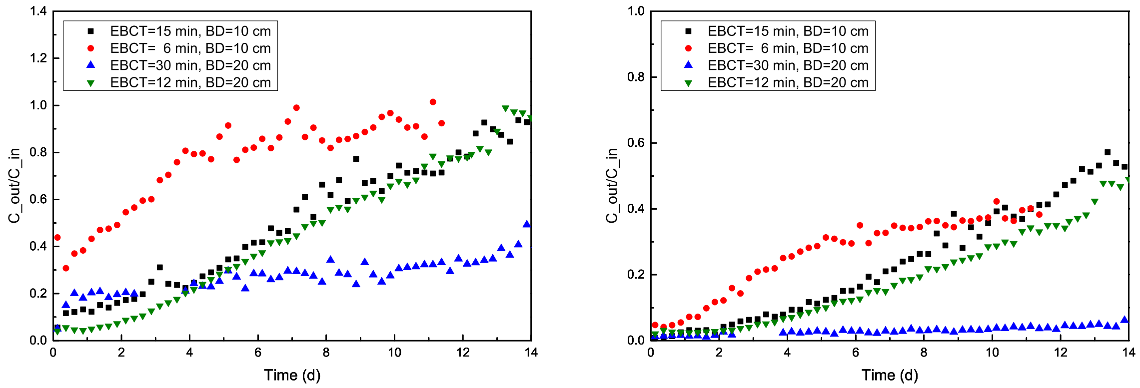

(a) Benzotriazole (b) Methyl-benzotriazole

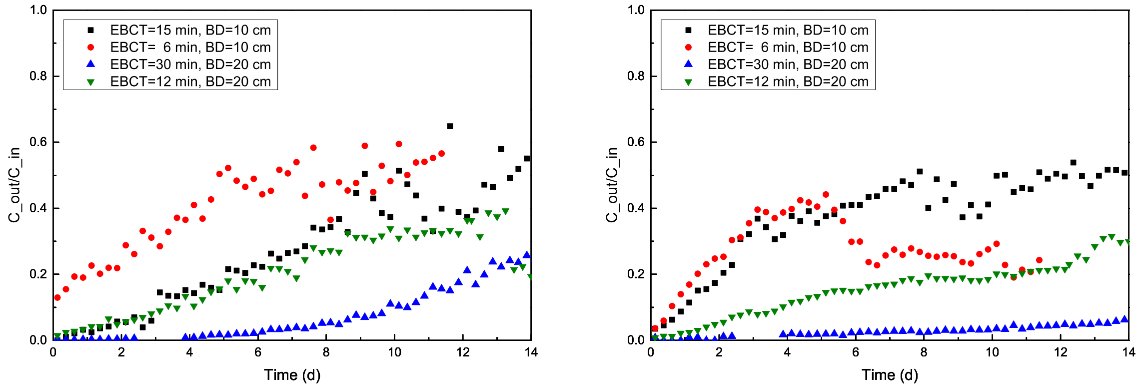

(c) Clarithromycin (d) Gabapentin

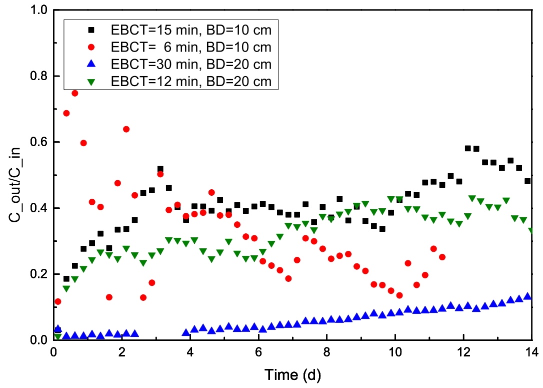

(e) Caffeine

Figure 3.12: Breakthrough curves for OMP adsorption in zeolite packed columns in WW at different of EBCTs and bed depths (I)

Figure 3.13 showed a fairly early breakthrough within 3-8 days for carbamazepine, sulfamethoxazole, diclofenac, clofibric acid, and theophylline. It was insufficient to remove these five OMPs in BEA zeolite packed columns.

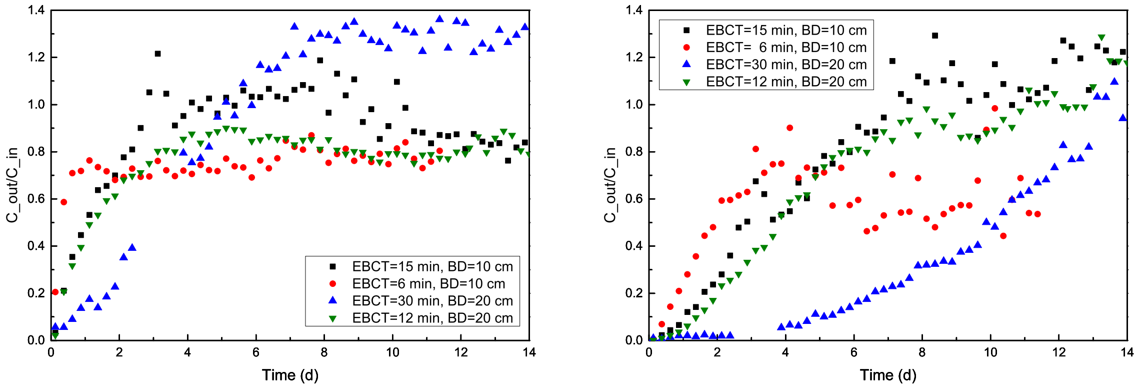

(a) Carbamazepine (b) Sulfamethoxazole

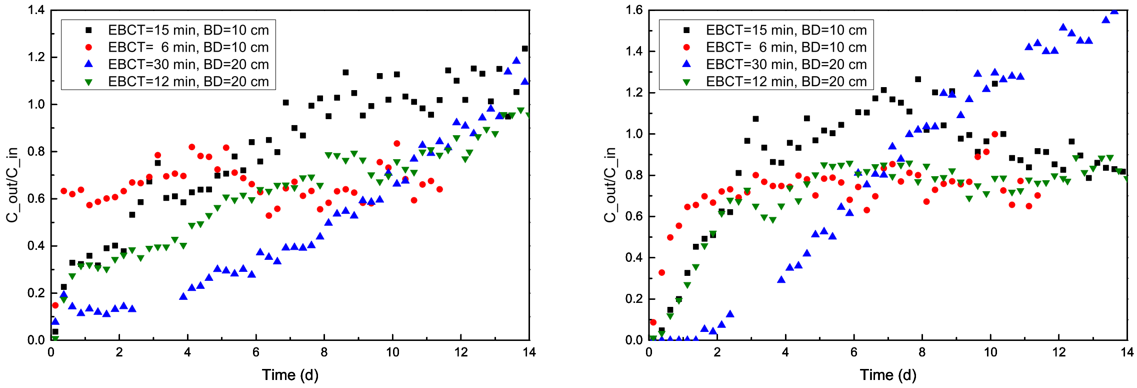

(c) Diclofenac (d) Clofibric acid

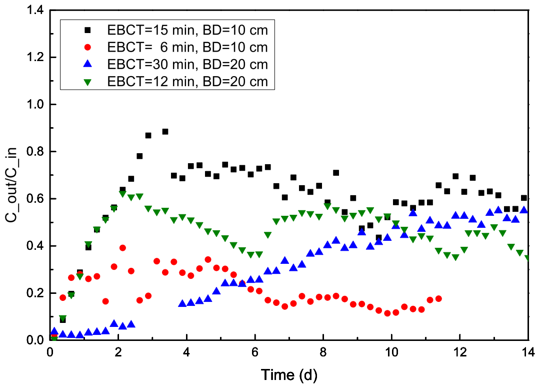

(e) Theophylline

Figure 3.13: Breakthrough curves for OMP adsorption in zeolite packed columns in WW at different of EBCTs and bed depths (II)

In conclusion, the zeolite packed columns were effective in removing 12 of the 18 target OMPs in this study. (The breakthrough of hydrochlorothiazide was not investigated due to unavailable experimental data.) With an EBCT of 12 or 15 min, the appropriate operation time is approximately 10 days, which means that it is necessary to renew the column every 10 days to ensure its performance.

3.3.7. DOC, UV-254 and ion concentration in WW

DOC and UV-254 in the influent and effluent of columns were measured during the column experiments (Figure 3.14). DOC in influent of four groups of column experiments was in the range of 6.6-10.6 mg/L. The removal efficiencies of DOC in columns were in the range of 4%-20%. The initial UV-254 ranged from 0.19 to 0.28. The reduction of UV-254 in columns ranged from 2% to 16%. DOC and UV-254 are good indicators for organic matters. It is illustrated that only a small part of organic matters was adsorbed by zeolite packed column. As discussed earlier, NOMs were not adsorbed by zeolite due to their large molecular size. These adsorbed organic matters were probably different OMPs present in WWTPs, which can be adsorbed by zeolite packed columns.

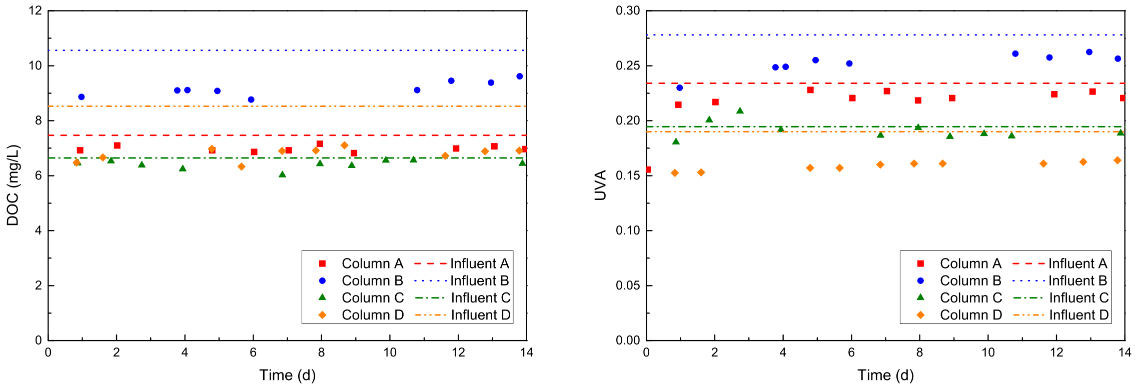

(a) DOC

(b) UV-254

Figure 3.14: DOC and UV-254 in the inlet and outlet of columns

Ions in the influent and effluent of columns were analyzed during the column experiments, including four cations (Na^+, K^+, Mg^{2+}, Ca^{2+}) and three anions (Cl^-, NO_3^-, SO_4^{2-}). As shown in Figure 3.16 and 3.15, most of the concentration of ions were stable during the 14 days. The ion concentrations in effluent were close to the influent concentration. It is assumed that ions quickly reached the complete breakthrough within 1 day before the first sampling.

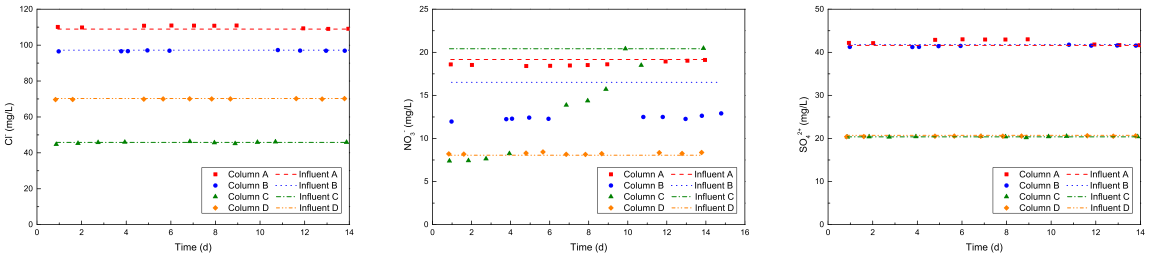

(a) Cl^-

(b) NO_3^-

(c) SO_4^{2-}

Figure 3.15: Anions in the inlet and outlet of columns

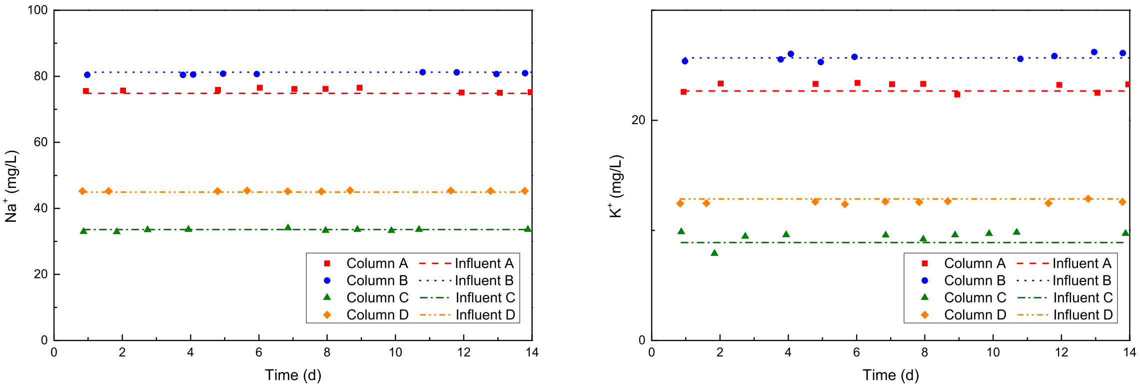

(a) Na$^+$ (b) K$^+$

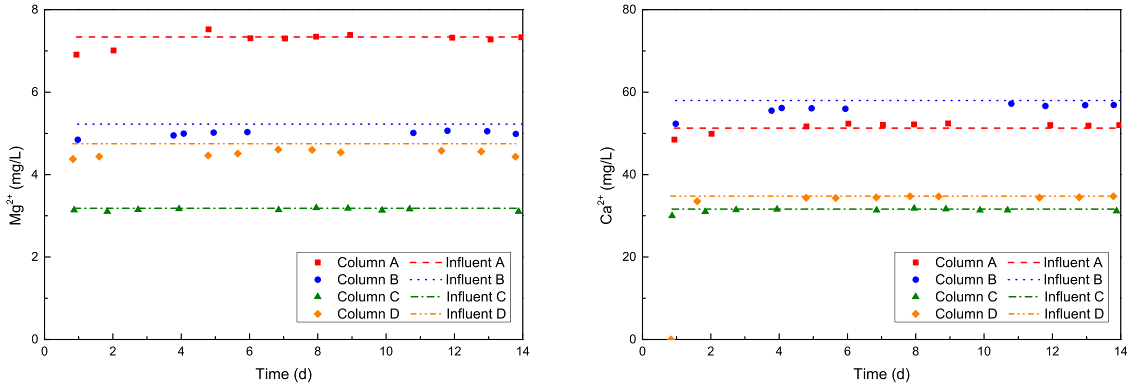

(c) Mg^{2+} (d) Ca^{2+}

Figure 3.16: Cations in the inlet and outlet of columns

3.4. Prediction of breakthrough curves

In this section, breakthrough curves for OMP adsorption in DW and WW were simulated by Comsol Multiphysics software with the isotherm and kinetic constants. The simulated results were compared with experimental data. Sensitivity analysis of the model was implemented to discover the effect of the variables systematically.

3.4.1. Parameter settings

To measure the axial dispersion coefficient (D_L) of the zeolite packed column, NaCl solution was fed to the column and the conductivity of the effluent was measured to obtain a breakthrough curve. The adsorption of NaCl by zeolites was ignored. The model was developed earlier, where D_L was achieved by fitting the simulated breakthrough curve to experimental data. Figure 3.17 illustrates the fitting results. Higher velocity resulted in faster axial dispersion.

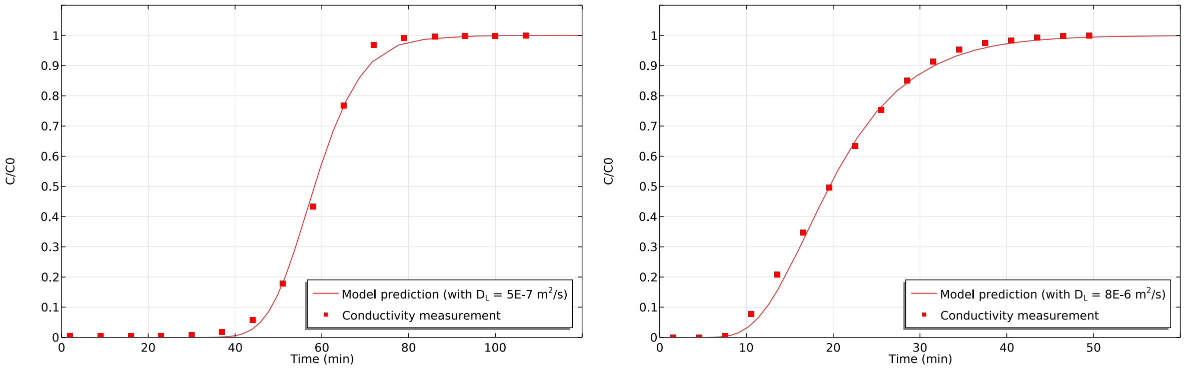

(a) v = 1.67 cm/min

(b) v = 0.67 cm/min

Figure 3.17: Measured and simulated breakthrough curves of NaCl in columns under two different velocities

The density and porosity of zeolite packed column were measured. 32.04 g zeolite granules got wet and were dosed in a volumetric cylinder partially filled with water. All the zeolites were below the water surface and the added volumetric scale showed the particle volume, which is 30.0 ml. Then, the particle density was calculated, which is 1.068 g/ml. The packed volume of 32.04 g zeolite granules in the column is 28.06 ml. The bulk density could be obtained, which is 0.571 g/ml. Based on the particle and bulk density, porosity could be calculated with the result of 0.465.

Besides the parameters listed in Table 3.5, linear isotherm constants in Appendix B and PFO kinetic constants in section 3.2 were required in model implementation.

Table 3.5: Parameters in model

Parameters	**Units**	**Values**	
Porosity (ep)	[-]	0.465	
Bulk density (rho_b)	[g/ml]	0.571	
Particle density (rho_p)	[g/ml]	1.068	
Superficial velocity (v)	[cm/min]	1.67	0.67
Axial dispersion coefficient (D_L)	[m^2/s]	8.0e-6	5.0E-7

3.4.2. Simulation results

To evaluate the performance of prediction model, simulation results were compared with experimental data. The breakthrough curves can be predicted only for OMPs with valid isotherm constants and kinetic constants, which are shown in the section below.

The experimental and simulated breakthrough curves of benzotriazole, carbamazepine, caffeine and theophylline in DW were compared in Figure 3.18. The concentration ratios $C/C0$ of the four OMPs followed a consistent order in the experimental and simulated breakthrough curves: carbamazepine > theophylline > caffeine > benzotriazole. In the results with EBCT of 6 min, the experimental and simulated breakthrough curves had similar slopes while the starting points were quite different. In DW, the simulation with a velocity of 1.67 ml/min had an overestimated breakthrough, while the simulation with a velocity of 0.67 ml/min had an underestimated breakthrough. These experimental breakthrough curves all started from a point close to zero.

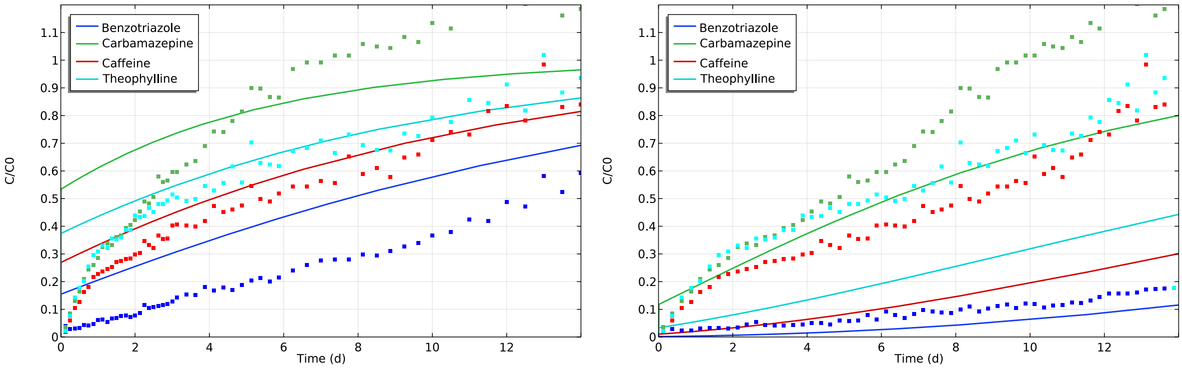

(a) v = 1.67 cm/min, bed depth = 10 cm

(b) v = 0.67 cm/min, bed depth = 10 cm

Figure 3.18: Experimental and simulated breakthrough curves in DW

It is assumed that the actual kinetic constants k in the columns were much larger than those in the batch experiments. In most adsorption processes, the controlling step is either film diffusion or intraparticle diffusion. High fluid velocity can reduce or even eliminate film mass transfer resistance, while small particle size implies low intraparticle diffusion resistance (Yao and Chen, 2017). By using 3-fold kinetic constants, the results of the prediction model were shown in Figure 3.19. The breakthrough curves for carbamazepine, caffeine and theophylline with a velocity of 1.67 cm/min were well matched with the promoted simulation results. Simulations with a velocity of 0.67 cm/min did not perform well enough.

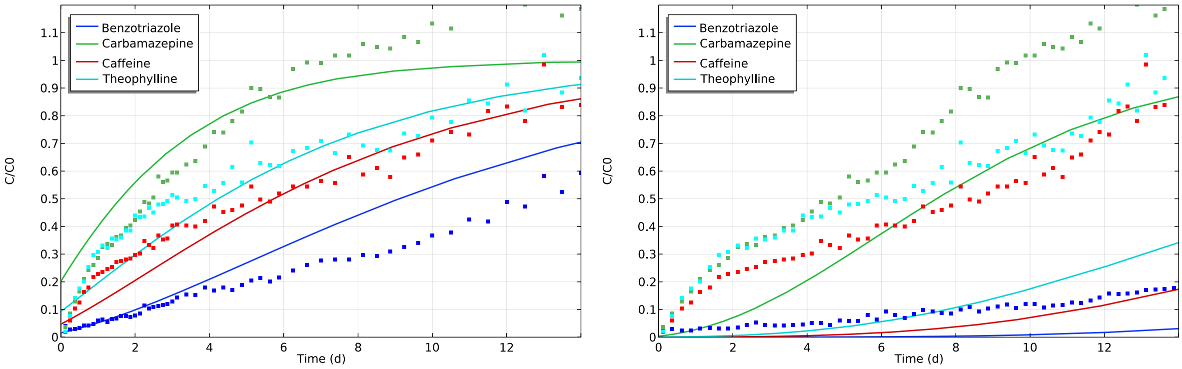

(a) v = 1.67 cm/min, bed depth = 10 cm

(b) v = 0.67 cm/min, bed depth = 10 cm

Figure 3.19: Experimental and simulated breakthrough curves in DW using 3-fold kinetic constants

The experimental and simulated breakthrough curves of benzotriazole, methyl-benzotriazole, carbamazepine and sulfamethoxazole in WW were compared in Figure 3.20. The concentration ratios $C/C0$ of the four OMPs followed the same order in the experimental and simulated breakthrough curves, which was carbamazepine > sulfamethoxazole > benzotriazole > methyl-benzotriazole.

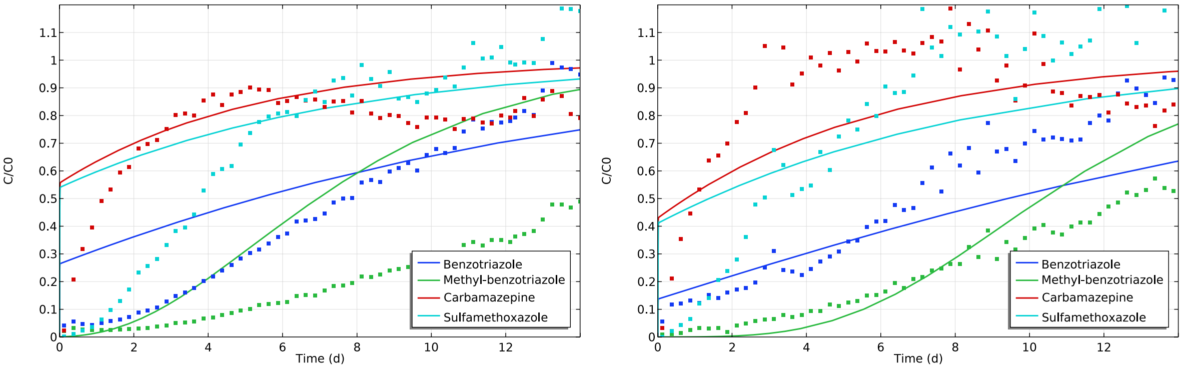

(a) v = 1.67 cm/min, bed depth = 20 cm

(b) v= 0.67 ml/min, bed depth = 10 cm

Figure 3.20: Experimental and simulated breakthrough curves in WW

Consistent with the scaling up of the kinetic rates in the prediction model in DW, the promoted simulation results in WW were shown in Figure 3.19 by using 3-fold kinetic constants. With larger kinetic constants, the starting points of the simulated breakthrough curves in WW were closer to the actual experimental values. The promoted prediction of the breakthrough curves for carbamazepine and sulfamethoxazole was in better agreement with the experimental breakthrough. The simulation of the breakthrough curves for benzotriazole was improved at a velocity of 1.67 cm/min, but not at a velocity of 0.67 cm/min. The breakthrough curves for methyl-benzotriazole were well matched at a velocity of 0.67 cm/min, but poorly matched at a velocity of 1.67 cm/min.

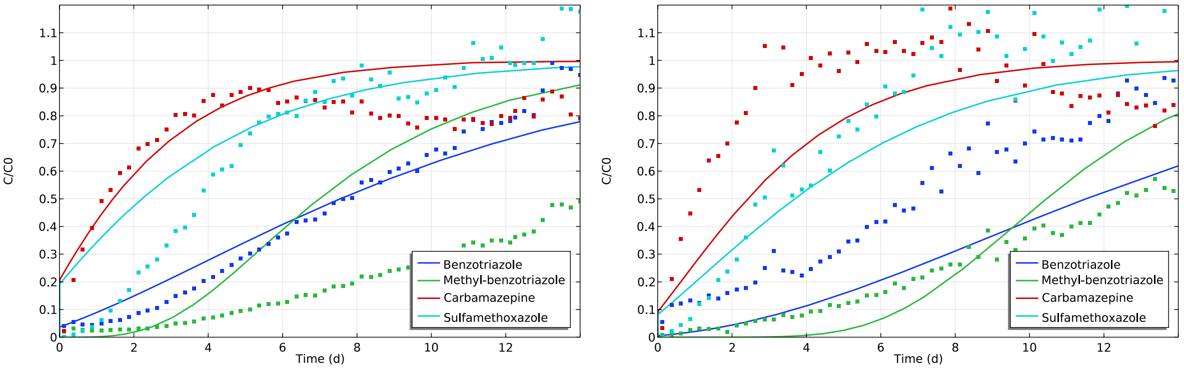

(a) v = 1.67 cm/min, bed depth = 20 cm

(b) v = 0.67 cm/min, bed depth = 10 cm

Figure 3.21: Experimental and simulated breakthrough curves in WW using 3-fold kinetic constants

Additionally, the prediction model did not take into account the desorption of OMPs from zeolite columns after saturation. The simulated curves always ended at 1 (C/C0), while some experimental breakthrough curves ended at values above 1.

In summary, expanding the kinetic constants obtained from the batch experiments makes the shape of the simulated breakthrough curve more similar to the actual situation. The exact relationship between the kinetics in the columns and in the batch experiments needs further investigation.

3.4.3. Sensitivity analysis

Single-parameter sensitivity analysis was performed to investigate the influences of isotherm constants, kinetic constants, dispersion coefficient, and porosity on the breakthrough curves in columns. The breakthrough curve of benzotriazole with the EBCT of 15 min and the bed depth of 10 cm in WW was chosen as the example. The results are shown in Figure 3.22.

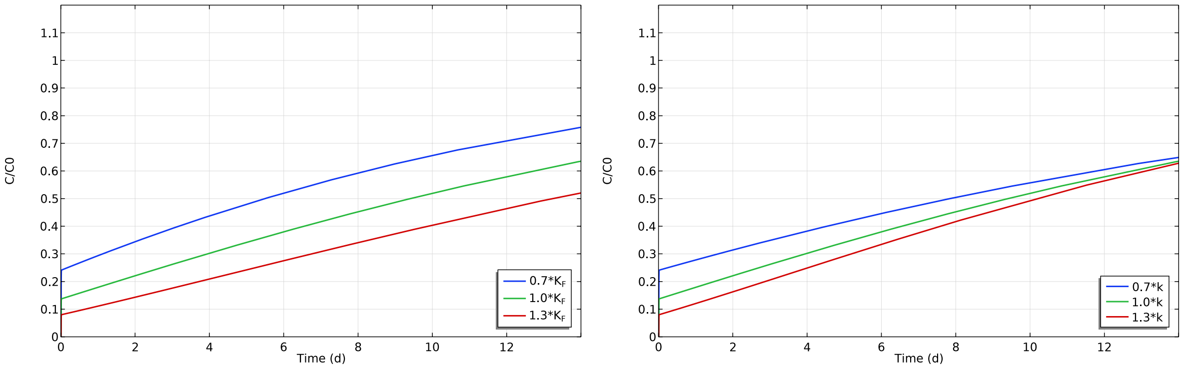

(a) Isotherm constants (b) Kinetic constants

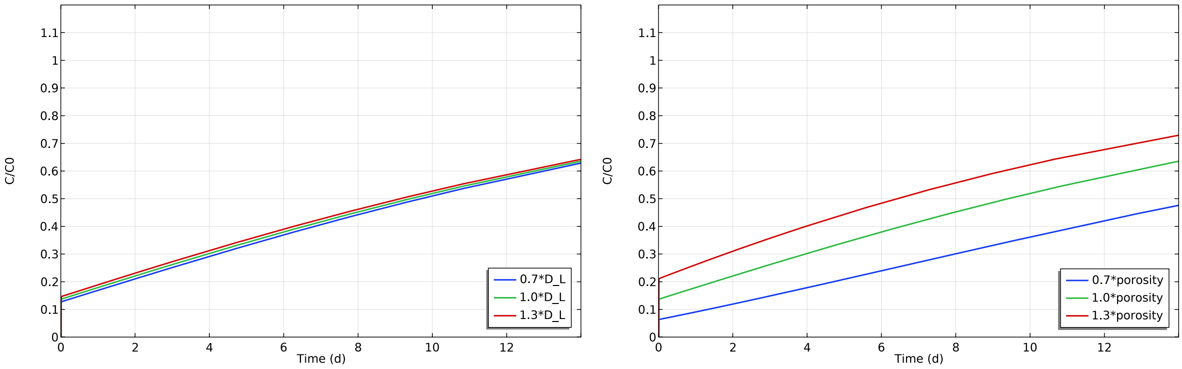

(c) Dispersion coefficient (d) Porosity

Figure 3.22: Sensitivity analysis of the prediction model

With the parameters varied by ±30%, it could be investigated that isotherm constants and porosity had a significant impact on the prediction model of breakthrough curves. Dispersion coefficient had a minimal impact on the model.

From the figure, it is indicated that a larger isotherm constant leads to a slower breakthrough. A larger isotherm constant means that zeolite has a larger adsorption capacity of the specific OMP. Under the same experimental conditions, the OMP will saturate in the column for longer time. A larger kinetic constant means a faster adsorption rate, which leads to a greater slope of the breakthrough curves.

The dispersion coefficient in zeolite columns in other studies were 8.1×10^{-7}-1.4×10^{-6} m^2/s (Ma et al., 2020) and 1.4×10^{-9}-7.7×10^{-8} m^2/s (Markovska et al., 2001). A change in the order of magnitude of the dispersion coefficient can significantly affect the breakthrough curve. The Peclet number is smaller with a larger dispersion coefficient, which means the motion of OMPs is determined largely by advection rather than diffusion. Under smaller Peclet number conditions, fewer OMPs can enter the internal site of zeolite through the water film. Poursaeidesfahani et al. (2019) reported similar results that a higher dispersion coefficient made a more gradual breakthrough curve.

The figure shows that a larger porosity leads to poor adsorption. This can be explained by the less packing weight of zeolite granules in the column system with a larger porosity. Fewer adsorption sites on zeolite give a faster breakthrough.

3.4.4. Prediction of the adsorption by zeolite packed columns with different operational parameters

Supplementary predictions of the breakthrough curves in zeolite packed columns were carried out for OMPs with appropriate isothermal constants. The model was predicted for 7 days at the EBCT of 15 min and 7 min, respectively. Among the 8 OMPs, only benzotriazole and diclofenac showed increasing breakthrough curves. These two compounds had endpoints of $C/C0$ below 0.5 at 15 min EBCT, and at approximately 0.7 at 7 min EBCT. The other six OMPs, metoprolol, propranolol, sotalol, trimethoprim, ketoprofen and sulfadimethoxine, did not show increasing breakthrough curves over, implying that they would be perfectly removed within 7 days.

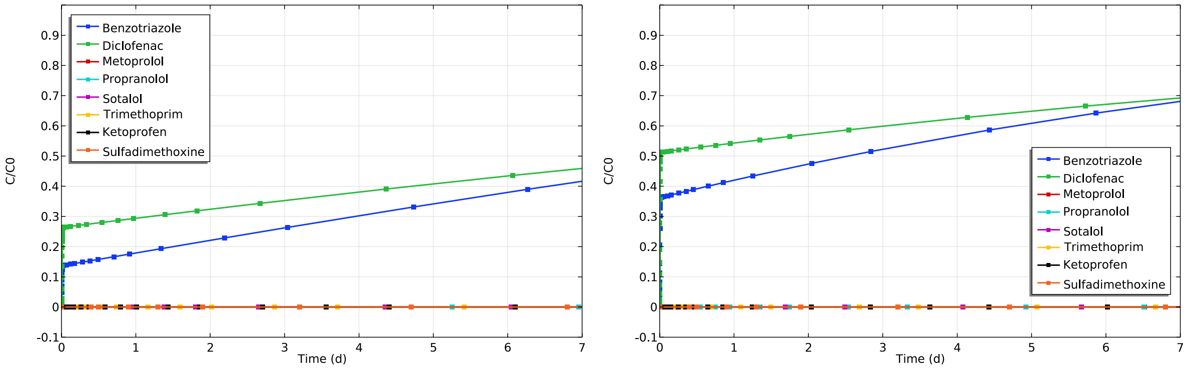

(a) EBCT = 15 min (b) EBCT = 7 min

Figure 3.23: Prediction of the breakthrough curves at the EBCT of 15 min and 7 min

The prediction results can provide recommendations for the design of zeolite packed columns for OMP treatment in WWTP. 7-15 minutes is an optional range of EBCT settings for a larger scaled column to remove the 8 OMPs sufficiently.

4

Conclusion

In this research, the adsorption of 18 target OMPs by zeolite granules was fully studied in batch and column experiments. The adsorption capacity and kinetics of OMPs in DW and secondary effluent from WWTP (WW matrix) were investigated. A prediction model of OMP breakthrough curves in zeolite packed columns was established and evaluated.

The factors influencing OMP adsorption by zeolite granules in batch and column experiments are OMP species, water matrices, and operational parameters:

- Positively charged OMPs were better adsorbed by zeolite granules than neutral and negatively charged OMPs.
- Background matrices in the WW matrix (secondary effluent from WWTP) reduced the adsorption capacity and kinetics of most OMPs, and made faster breakthroughs in columns. On the contrary, a few negatively charged OMPs, such as diclofenac and clofibric acid, showed stronger adsorption capacity and kinetics in the WW matrix.
- Higher zeolite dosage resulted in faster kinetics of OMP adsorption.

Column experiments showed that 12 of the 18 target OMPs could be effectively removed at the EBCT of 12 min, achieving removal efficiencies of 50% over 10 days. Carbamazepine, diclofenac, sulfamethoxazole, clofibric acid and theophylline were poorly removed in the zeolite packed column.

The mathematic model for the prediction of OMP breakthrough curves was optimized. Predicted breakthrough curves fitted experimental breakthrough curves better by applying larger kinetic constants. It indicated that the adsorption kinetic of OMPs in columns was underestimated by the adsorption kinetic parameters from the batch experiment. It was predicted an EBCT of 15 min is an alternative for a 7-day operation to remove OMPs sufficiently by zeolite packed columns.

5

Limitations and suggestions

In batch experiments, a few OMPs, such as carbamazepine, sulfamethoxazole and clofibric acid, had invalid isotherm results since their equilibrium concentrations were close to initial concentrations. To improve the results, it is recommended to dose more zeolite for greater removal.

In batch experiments containing OMP mixtures, there are always compounds with the best removal (equilibrium concentrations below detection limits) and worst removal (equilibrium concentrations close to initial concentrations), for which isotherm results are difficult to obtain. If necessary, using a separate OMP solution with an appropriate range of zeolite dosage may be an option to obtain isotherms. It should be noticed that the isotherms obtained in a single OMP solution do not take into account the competition between the different OMPs.

In kinetic experiments, a few OMPs were biodegraded before reaching equilibrium, and their kinetic results were not available. For biodegradable OMPs, it is preferable to dose more zeolite granules so that they can reach equilibrium before biodegradation occurs. In this way, a reliable q_e could be obtained from experimental data, and then an accurate k can be obtained by curve fitting. A few OMPs, such as carbamazepine and clofibric acid, had poor kinetic results due to their low removal rate. It is suggested that better kinetic results may be obtained by increasing the dosage of zeolite.

From the column experiments, it is known that renewing the zeolite packed column every 10 days at an EBCT of 12 minutes could provide a robust and effective treatment system for the removal of the 12 target OMPs. Using a column with a fixed tube diameter, slower flow velocities will improve removal efficiency, but will reduce the inlet flow. Larger bed depths will promote adsorption performance, but will scale up the installations. The design of the column should be optimized for cost-effectiveness based on the target capacity and available footprint.

In the modelling part, the model simulated the variation of C/C0 from 0 to 1. In practice, the experimental data showed that some OMPs have a C/C0 above 1, which is due to desorption occurring after saturation. The prediction model did not take into account the post-saturation behaviour and the effect of desorbed compounds on other compounds. Additionally, the predicted breakthrough curve with 3-fold kinetic constants obtained from batch experiments showed a better match to the experimental data. Further research on the adsorption kinetics at different hydraulic conditions was recommended.

This study investigated how the WW matrix from WWTP effluent affected the adsorption of OMP by zeolite granules, but did not specify which component of the effluent matrix influenced the adsorption behaviour. It is suggested to carry out more experiments in demi-water with the addition of quantitative components (e.g.,inorganic ions or NOMs) that may influence OMP adsorption.

Bibliography

Laila Abu-Lail, John A Bergendahl, and Robert W Thompson. Adsorption of methyl tertiary butyl ether on granular zeolites: batch and column studies. *Journal of hazardous materials*, 178(1-3): 363–369, 2010.

PG Aguilera and FJ Gutiérrez Ortiz. Prediction of fixed-bed breakthrough curves for h2s adsorption from biogas: Importance of axial dispersion for design. *Chemical Engineering Journal*, 289:93–98, 2016.

K Aoki and Y Adachi. Kinetics of polyelectrolyte adsorption onto polystyrene latex particle studied using electrophoresis: effects of molecular weight and ionic strength. *Journal of colloid and interface science*, 300(1):69–77, 2006.

Muhammad Arslan, Inaam Ullah, Jochen A Müller, Naeem Shahid, and Muhammad Afzal. Organic micropollutants in the environment: ecotoxicity potential and methods for remediation. *Enhancing cleanup of environmental pollutants*, pages 65–99, 2017.

Olivier Autin, Christophe Romelot, Lena Rust, Julie Hart, Peter Jarvis, Jitka MacAdam, Simon A Parsons, and Bruce Jefferson. Evaluation of a uv-light emitting diodes unit for the removal of micropollutants in water for low energy advanced oxidation processes. *Chemosphere*, 92(6): 745–751, 2013.

Ahmed Amine Azzaz, Salah Jellali, Rahma Souissi, Karim Ergaieg, and Latifa Bousselmi. Alkaline-treated sawdust as an effective material for cationic dye removal from textile effluents under dynamic conditions: breakthrough curve prediction and mechanism exploration. *Environmental Science and Pollution Research*, 24(22):18240–18256, 2017.

Abhijit Chatterjee and Silke Schiewer. Biosorption of cadmium (ii) ions by citrus peels in a packed bed column: effect of process parameters and comparison of different breakthrough curve models. *CLEAN–Soil, Air, Water*, 39(9):874–881, 2011.

A Chojnacki, Katarzyna Chojnacka, J Hoffmann, and H Gorecki. The application of natural zeolites for mercury removal: from laboratory tests to industrial scale. *Minerals Engineering*, 17(7-8):933–937, 2004.

Kangmin Chon, Sarper Sarp, Sungyun Lee, Jong-Hoon Lee, JA Lopez-Ramirez, and Jaeweon Cho. Evaluation of a membrane bioreactor and nanofiltration for municipal wastewater reclamation: Trace contaminant control and fouling mitigation. *Desalination*, 272(1-3):128–134, 2011.

European Commission. Directive 2008/105/ec of the european parliament and of the council on environmental quality standards in the field of water policy, amending and subsequently repealing council directives 82/176/eec, 83/513/eec, 84/156/eec, 84/491/eec, 86/280/eec and amending directive 2000/60/ec of the european parliament and of the council. *Off. J. Eur. Union*, 51:84–97, 2008.

European Commission. European commission implementation decision 2015/495/ec establishing a watch list of substances for union-wide monitoring in the field of water policy pursuant to directive 2008/105/ec of the european parliament and of the councily. *Off. J. Eur. Union*, 58:40–42, 2015.

European Commission. European commission implementation decision 2018/840 establishing a watch list of substances for union-wide monitoring in the field of water policy pursuant to directive 2008/105/ec of the european parliament and of the council and repealing commission implementing decision (eu) 2015/495. *Off. J. Eur. Union*, 61:9–12, 2018.

Josef V Datel and Anna Hrabankova. Pharmaceuticals load in the svihov water reservoir (czech republic) and impacts on quality of treated drinking water. *Water*, 12(5):1387, 2020.

Matthias De Cazes, Ricardo Abejón, Marie-Pierre Belleville, and José Sanchez-Marcano. Membrane bioprocesses for pharmaceutical micropollutant removal from waters. *Membranes*, 4(4):692–729, 2014.

N De la Cruz, J Giménez, S Esplugas, D Grandjean, LF De Alencastro, and César Pulgarin. Degradation of 32 emergent contaminants by uv and neutral photo-fenton in domestic wastewater effluent previously treated by activated sludge. *Water research*, 46(6):1947–1957, 2012.

David J De Ridder, JQJC Verberk, Sebastiaan GJ Heijman, Gary L Amy, and Johannis C Van Dijk. Zeolites for nitrosamine and pharmaceutical removal from demineralised and surface water: mechanisms and efficacy. *Separation and purification technology*, 89:71–77, 2012.

E Demirbas, M Kobya, and MT Sulak. Adsorption kinetics of a basic dye from aqueous solutions onto apricot stone activated carbon. *Bioresource technology*, 99(13):5368–5373, 2008.

E Demirbas, N Dizge, MT Sulak, and M Kobya. Adsorption kinetics and equilibrium of copper from aqueous solutions using hazelnut shell activated carbon. *Chemical Engineering Journal*, 148(2-3): 480–487, 2009.

Camilla Di Marcantonio, Agostina Chiavola, Simona Dossi, Giancarlo Cecchini, Simone Leoni, Alessandro Frugis, Massimo Spizzirri, and Maria Rosaria Boni. Occurrence, seasonal variations and removal of organic micropollutants in 76 wastewater treatment plants. *Process Safety and Environmental Protection*, 141:61–72, 2020.

JC Dijt, MA Cohen Stuart, JE Hofman, and GJ Fleer. Kinetics of polymer adsorption in stagnation point flow. *Colloids and surfaces*, 51:141–158, 1990.

Leila Dolatyari, Mohammad Reza Yaftian, and Sadegh Rostamnia. Fixed-bed column dynamic studies and breakthrough curve analysis of eu (iii) ion adsorption onto chemically modified sba-15 silica materials. *Separation Science and Technology*, 52(3):393–403, 2017.

Rik IL Eggen, Juliane Hollender, Adriano Joss, Michael Schärer, and Christian Stamm. Reducing the discharge of micropollutants in the aquatic environment: the benefits of upgrading wastewater treatment plants, 2014.

Michael Fischer. Simulation-based evaluation of zeolite adsorbents for the removal of emerging contaminants. *Materials Advances*, 1(1):86–98, 2020.

Keng Yuen Foo and Bassim H Hameed. Insights into the modeling of adsorption isotherm systems. *Chemical engineering journal*, 156(1):2–10, 2010.

V Gabet-Giraud, Cecile Miege, R Jacquet, and Marina Coquery. Impact of wastewater treatment plants on receiving surface waters and a tentative risk evaluation: the case of estrogens and beta blockers. *Environmental Science and Pollution Research*, 21(3):1708–1722, 2014.

Peghah Ghomashi, Amir Charkhi, Mohammad Kazemeini, and Taher Yousefi. Removal of fluoride from wastewater by natural and modified nano clinoptilolite zeolite. *Journal of Water and Environmental Nanotechnology*, 5(3):270–282, 2020.

DP Grover, JL Zhou, PE Frickers, and JW Readman. Improved removal of estrogenic and pharmaceutical compounds in sewage effluent by full scale granular activated carbon: impact on receiving river water. *Journal of Hazardous Materials*, 185(2-3):1005–1011, 2011.

S.G.J. Heijman, W. Siegers, R. Sterk, and R. Hopman. Prediction of breakthrough of pesticides in GAC-filters and breakthrough of colour in ion-exchange-filters. *Water Supply*, 2(1):103–108, 2002.

YS Ho and G McKay. The kinetics of sorption of basic dyes from aqueous solution by sphagnum moss peat. *The Canadian journal of chemical engineering*, 76(4):822–827, 1998.

Rong Hu. Adsorption of organic micro-pollutants by zeolite granules: Batch and column studies. Master's thesis, Delft University of Technology, 2020. URL `http://resolver.tudelft.nl/uuid:269fbf06-6714-436c-852f-bd99e0ee7c1a`.

H-W Hung, T-F Lin, C Baus, F Sacher, and HJ Brauch. Competitive and hindering effects of natural organic matter on the adsorption of mtbe onto activated carbons and zeolites. *Environmental technology*, 26(12):1371–1382, 2005.

Ikechukwu A Ike, Tanju Karanfil, Jinwoo Cho, and Jin Hur. Oxidation byproducts from the degradation of dissolved organic matter by advanced oxidation processes–a critical review. *Water research*, 164: 114929, 2019.

Hilary I Inyang, Adrianna Onwawoma, and Sunyoung Bae. The elovich equation as a predictor of lead and cadmium sorption rates on contaminant barrier minerals. *Soil and Tillage Research*, 155: 124–132, 2016.

Cheng Jiang, Liyue Jia, Yiliang He, Bo Zhang, George Kirumba, and Jie Xie. Adsorptive removal of phosphorus from aqueous solution using sponge iron and zeolite. *Journal of colloid and interface science*, 402:246–252, 2013.

Nan Jiang, Ran Shang, Sebastiaan GJ Heijman, and Luuk C Rietveld. High-silica zeolites for adsorption of organic micro-pollutants in water treatment: A review. *Water research*, 144:145–161, 2018.

Nan Jiang, Ran Shang, Sebastiaan GJ Heijman, and Luuk C Rietveld. Adsorption of triclosan, trichlorophenol and phenol by high-silica zeolites: Adsorption efficiencies and mechanisms. *Separation and Purification Technology*, 235:116152, 2020.

Helen Kalavathy, B Karthik, and Lima Rose Miranda. Removal and recovery of ni and zn from aqueous solution using activated carbon from hevea brasiliensis: Batch and column studies. *Colloids and surfaces B: Biointerfaces*, 78(2):291–302, 2010.

Anthony M Kennedy and R Scott Summers. Effect of dom size on organic micropollutant adsorption by gac. *Environmental science & technology*, 49(11):6617–6624, 2015.

Mohamed Khalid, Guy Joly, Arlette Renaud, and Patrick Magnoux. Removal of phenol from water by adsorption using zeolites. *Industrial & Engineering Chemistry Research*, 43(17):5275–5280, 2004.

Sunil Kommineni, Jeffrey Zoeckler, Andrew Stocking, PS Liang, Amparo Flores, Rey Rodriguez, T Brown, R Per, and Anthony Brown. 3.0 advanced oxidation processes. *center for groundwater restoration and protection national water research institute*, 2000.

Bachar Koubaissy, Guy Joly, Isabelle Batonneau-Gener, and Patrick Magnoux. Adsorptive removal of aromatic compounds present in wastewater by using dealuminated faujasite zeolite. *Industrial & Engineering Chemistry Research*, 50(9):5705–5713, 2011.

Lubomira Kovalova, Hansruedi Siegrist, Urs Von Gunten, Jakob Eugster, Martina Hagenbuch, Anita Wittmer, Ruedi Moser, and Christa S McArdell. Elimination of micropollutants during post-treatment of hospital wastewater with powdered activated carbon, ozone, and uv. *Environmental science & technology*, 47(14):7899–7908, 2013.

Yunho Lee, Lubomira Kovalova, Christa S McArdell, and Urs von Gunten. Prediction of micropollutant elimination during ozonation of a hospital wastewater effluent. *Water research*, 64:134–148, 2014.

Yi Li, Tai-Shung Chung, Chun Cao, and Santi Kulprathipanja. The effects of polymer chain rigidification, zeolite pore size and pore blockage on polyethersulfone (pes)-zeolite a mixed matrix membranes. *Journal of Membrane Science*, 260(1-2):45–55, 2005.

Robert Loos, Raquel Carvalho, Diana C António, Sara Comero, Giovanni Locoro, Simona Tavazzi, Bruno Paracchini, Michela Ghiani, Teresa Lettieri, Ludek Blaha, et al. Eu-wide monitoring survey on emerging polar organic contaminants in wastewater treatment plant effluents. *Water research*, 47 (17):6475–6487, 2013.

Yunlong Luo, Wenshan Guo, Huu Hao Ngo, Long Duc Nghiem, Faisal Ibney Hai, Jian Zhang, Shuang Liang, and Xiaochang C Wang. A review on the occurrence of micropollutants in the aquatic environment and their fate and removal during wastewater treatment. *Science of the total environment*, 473:619–641, 2014.

Jinxing Ma, Ruobin Dai, Mei Chen, Stuart J Khan, and Zhiwei Wang. Applications of membrane bioreactors for water reclamation: micropollutant removal, mechanisms and perspectives. *Bioresource technology*, 269:532–543, 2018.

Junchao Ma, Yong Wang, Geoffrey W Stevens, and Kathryn A Mumford. Hydrocarbon adsorption performance and regeneration stability of diphenyldichlorosilane coated zeolite and its application in permeable reactive barriers: Column studies. *Microporous and Mesoporous Materials*, 294:109843, 2020.

N Mansouriieh, MR Sohrabi, and M Khosravi. Adsorption kinetics and thermodynamics of organophosphorus profenofos pesticide onto fe/ni bimetallic nanoparticles. *International journal of environmental science and technology*, 13(5):1393–1404, 2016.

L Markovska, V Meshko, V Noveski, and M Marinkovski. Solid diffusion control of the adsorption of basic dyes onto granular activated carbon and natural zeolite in fixed bed columns. *Journal of the Serbian Chemical Society*, 66(7):463–475, 2001.

T Mathialagan and T Viraraghavan. Adsorption of cadmium from aqueous solutions by perlite. *Journal of Hazardous Materials*, 94(3):291–303, 2002.

F Meinel, AS Ruhl, A Sperlich, F Zietzschmann, and M Jekel. Pilot-scale investigation of micropollutant removal with granular and powdered activated carbon. *Water, Air, & Soil Pollution*, 226(1):1–10, 2015.

Silvio Montalvo, César Huiliñir, R Borja, E Sánchez, and C Herrmann. Application of zeolites for biological treatment processes of solid wastes and wastewaters–a review. *Bioresource technology*, 301:122808, 2020.

Norihide Nakada, Hiroyuki Shinohara, Ayako Murata, Kentaro Kiri, Satoshi Managaki, Nobuyuki Sato, and Hideshige Takada. Removal of selected pharmaceuticals and personal care products (ppcps) and endocrine-disrupting chemicals (edcs) during sand filtration and ozonation at a municipal sewage treatment plant. *Water research*, 41(19):4373–4382, 2007.

Luong N Nguyen, Faisal I Hai, Jinguo Kang, William E Price, and Long D Nghiem. Coupling granular activated carbon adsorption with membrane bioreactor treatment for trace organic contaminant removal: Breakthrough behaviour of persistent and hydrophilic compounds. *Journal of environmental management*, 119:173–181, 2013.

Ersin Polat, Mehmet Karaca, Halil Demir, and A Naci Onus. Use of natural zeolite (clinoptilolite) in agriculture. *Journal of fruit and ornamental plant research*, 12(1):183–189, 2004.

Ali Poursaeidesfahani, Eduardo Andres-Garcia, Martijn de Lange, Ariana Torres-Knoop, Marcello Rigutto, Nitish Nair, Freek Kapteijn, Jorge Gascon, David Dubbeldam, and Thijs JH Vlugt. Prediction of adsorption isotherms from breakthrough curves. *Microporous and Mesoporous Materials*, 277:237–244, 2019.

Emmanuel D Revellame, Dhan Lord Fortela, Wayne Sharp, Rafael Hernandez, and Mark Zappi. Adsorption kinetic modeling using pseudo-first order and pseudo-second order rate laws: A review. *Cleaner Engineering and Technology*, page 100032, 2020.

Ana R Lado Ribeiro, Nuno FF Moreira, Gianluca Li Puma, and Adrián MT Silva. Impact of water matrix on the removal of micropollutants by advanced oxidation technologies. *Chemical Engineering Journal*, 363:155–173, 2019.

Alírio E Rodrigues and Carlos Manuel Silva. What's wrong with lagergreen pseudo first order model for adsorption kinetics? *Chemical Engineering Journal*, 306:1138–1142, 2016.

Sara Rodriguez-Mozaz, Ivone Vaz-Moreira, Saulo Varela Della Giustina, Marta Llorca, Damià Barceló, Sara Schubert, Thomas U Berendonk, Irene Michael-Kordatou, Despo Fatta-Kassinos, Jose Luis Martinez, et al. Antibiotic residues in final effluents of european wastewater treatment plants and their impact on the aquatic environment. *Environment international*, 140:105733, 2020.

Sukanyah Shanmuganathan, Paripurnanda Loganathan, Christian Kazner, MAH Johir, and Saravanamuthu Vigneswaran. Submerged membrane filtration adsorption hybrid system for the removal of organic micropollutants from a water reclamation plant reverse osmosis concentrate. *Desalination*, 401:134–141, 2017.

Larissa LS Silva, Carolina G Moreira, Bianca A Curzio, Fabiana V da Fonseca, et al. Micropollutant removal from water by membrane and advanced oxidation processes—a review. *Journal of Water Resource and Protection*, 9(05):411, 2017.

Alexander Simon, Long Duc Nghiem, Pierre Le-Clech, Stuart J Khan, and Jörg E Drewes. Effects of membrane degradation on the removal of pharmaceutically active compounds (phacs) by nf/ro filtration processes. *Journal of Membrane Science*, 340(1-2):16–25, 2009.

Jean-Pierre Simonin and J Bouté. Intraparticle diffusion-adsorption model to describe liquid/solid adsorption kinetics. *Revista mexicana de ingeniería química*, 15(1):161–173, 2016.

S Sircar and JR Hufton. Why does the linear driving force model for adsorption kinetics work? *Adsorption*, 6(2):137–147, 2000.

J Stelzer, M Paulus, M Hunger, and J Weitkamp. Hydrophobic properties of all-silica zeolite beta. *Microporous and mesoporous materials*, 22(1-3):1–8, 1998.

Qian Sui, Jun Huang, Shubo Deng, Gang Yu, and Qing Fan. Occurrence and removal of pharmaceuticals, caffeine and deet in wastewater treatment plants of beijing, china. *Water research*, 44(2):417–426, 2010.

Selina Tisler and Christian Zwiener. Formation and occurrence of transformation products of metformin in wastewater and surface water. *Science of the Total Environment*, 628:1121–1129, 2018.

Md Tamez Uddin, Md Rukanuzzaman, Md Maksudur Rahman Khan, and Md Akhtarul Islam. Adsorption of methylene blue from aqueous solution by jackfruit (artocarpus heteropyllus) leaf powder: a fixed-bed column study. *Journal of environmental management*, 90(11):3443–3450, 2009.

Chung-Hsin Wu, Chao-Yin Kuo, and Shu-Shian Guan. Adsorption kinetics of lead and zinc ions by coffee residues. *Polish Journal of Environmental Studies*, 24(2), 2015.

Zhe Xu, Jian-guo Cai, and Bing-cai Pan. Mathematically modeling fixed-bed adsorption in aqueous systems. *Journal of Zhejiang University SCIENCE A*, 14(3):155–176, 2013.

Xin Yang, Riley C Flowers, Howard S Weinberg, and Philip C Singer. Occurrence and removal of pharmaceuticals and personal care products (ppcps) in an advanced wastewater reclamation plant. *Water research*, 45(16):5218–5228, 2011.

Chuncai Yao and Tianjiao Chen. A film-diffusion-based adsorption kinetic equation and its application. *Chemical Engineering Research and Design*, 119:87–92, 2017.

Xinyu Zheng, Nan Jiang, Huaili Zheng, Yuyang Wu, and Sebastiaan GJ Heijman. Predicting adsorption isotherms of organic micropollutants by high-silica zeolite mixtures. *Separation and Purification Technology*, page 120009, 2021.

A

Physiochemical property of OMPs

Name	Chemical formula	Molecular weight [g/mol]	Solubility [mg/mL]	Log D at pH = 7	Strongest acidic pKa	Strongest basic pKa	Charge at pH = 7	Projection radius	Chemical structure
Benzotriazole	$C_6H_5N_3$	119.13	7.3	1.29	9.04	0.22	-0.02	3.66-4.12	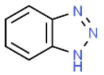
4-Methyl-1H-Benzotriazole	$C_7H_7N_3$	133.15	3.96	1.81	9.29	0.47	-0.01	4.05-4.43	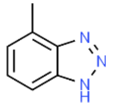
Carbamazepine	$C_{15}H_{12}N_2O$	236.27	0.04	2.77	15.96	-	0	4.48-5.76	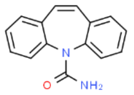
Diclofenac	$C_{14}H_{11}Cl_2NO_2$	296.15	15.1	1.37	4.15	-	-1.00	4.62-6.34	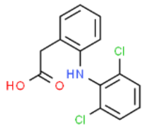
Hydrochlorothiazide	$C_7H_8ClN_3O_4S_2$	297.73	4.84	-0.58	9.09	-	-0.01	4.13-5.67	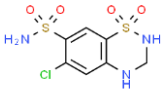
Metoprolol	$C_{15}H_{25}NO_3$	267.37	537.9	-0.81	14.09	9.67	+1.00	4.39-10.07	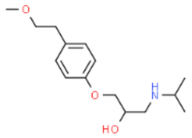
Sulfamethoxazole	$C_{10}H_{11}N_3O_3S$	253.28	12.6	0.14	6.16	1.97	-0.87	5.4-5.88	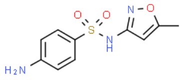
Propranolol	$C_{16}H_{21}NO_2$	259.35	24.1	0.02	14.09	9.67	+1.00	4.66-7.41	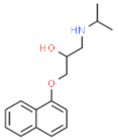
Sotalol	$C_{12}H_{20}N_2O_3S$	272.36	1273.5	-2.47	10.07	9.43	+0.99	4.21-7.94	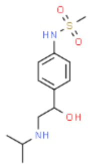
Trimethoprim	$C_{14}H_{18}N_4O_3$	290.32	1.1	0.92	-	7.16	+0.93	4.97-6.95	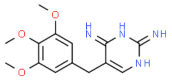

Name	**Chemical formula**	**Molecular weight [g/mol]**	**Solubility [mg/mL]**	**Log D at pH = 7**	**Strongest acidic pKa**	**Strongest basic pKa**	**Charge at pH = 7**	**Projection radius**	**Chemical structure**
Clarithromycin	$C_{38}H_{69}NO_{13}$	747.97	287.3	1.25	12.46	9	+0.99	7.38-9.46	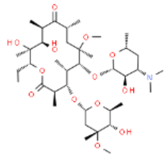
Ketoprofen	$C_{16}H_{14}O_3$	254.28	46.7	0.64	3.88	-	-1.00	4.37-6.58	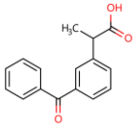
Clofibric Acid	$C_{10}H_{11}ClO_3$	214.65	214.6	-0.38	3.37	-	-1.00	3.5-6.2	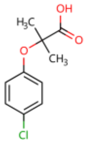
Sulfadimethoxine	$C_{12}H_{14}N_4O_4S$	310.33	0.18	0.97	6.91	1.99	-0.55	5.09-7.57	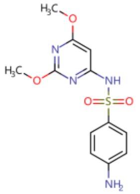
Caffeine	$C_8H_{10}N_4O_2$	194.19	70.9	-0.55	14.0	-1.16	0	4.44-5.03	
Theophylline	$C_7H_8N_4O_2$	180.17	22.74	-0.82	7.82	-0.78	-0.13	4.34-4.98	
Gabapentin	$C_9H_{17}NO_2$	171.24	12.8	-1.27	4.63	9.91	0	4.14-4.99	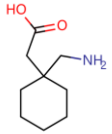
Metformin	$C_4H_{11}N_5$	129.17	8301.5	-5.70	-	12.3	+2.00	3.79-4.88	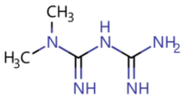

B

Linear and Freundlich isotherms of OMPs

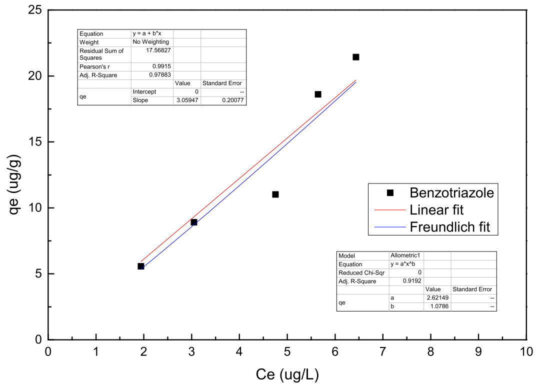

Equation	y = a + b*x		
Weight	No Weighting		
Residual Sum of Squares	17.56827		
Pearson's r	0.9915		
Adj. R-Square	0.97883		
		Value	Standard Error
qe	Intercept	0	--
	Slope	3.05947	0.20077

Model	Allometric1		
Equation	y = a*x^b		
Reduced Chi-Sqr	0		
Adj. R-Square	0.9192		
		Value	Standard Error
qe	a	2.62149	--
	b	1.0786	--

(a) Benzotriazole

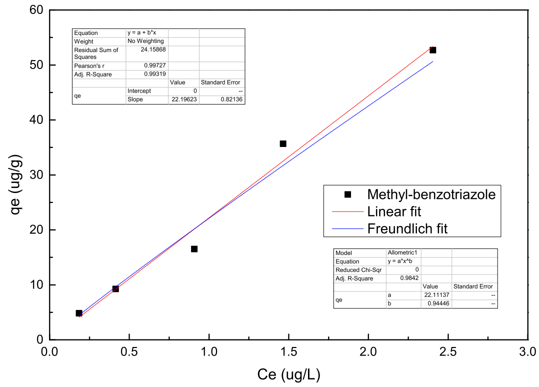

Equation	y = a + b*x		
Weight	No Weighting		
Residual Sum of Squares	24.15868		
Pearson's r	0.99727		
Adj. R-Square	0.99319		
		Value	Standard Error
qe	Intercept	0	--
	Slope	22.19623	0.82136

Model	Allometric1		
Equation	y = a*x^b		
Reduced Chi-Sqr	0		
Adj. R-Square	0.9842		
		Value	Standard Error
qe	a	22.11137	--
	b	0.94446	--

(b) Methyl-benzotriazole

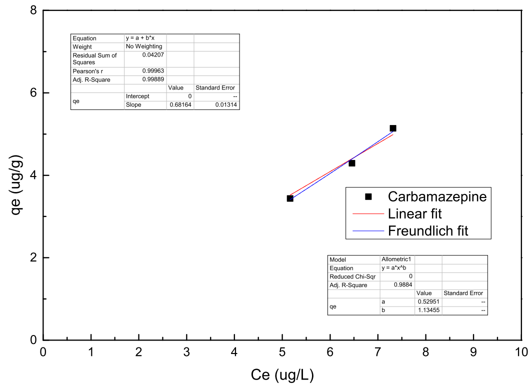

Equation	y = a + b*x		
Weight	No Weighting		
Residual Sum of Squares	0.04207		
Pearson's r	0.99963		
Adj. R-Square	0.99889		
		Value	Standard Error
qe	Intercept	0	--
	Slope	0.68164	0.01314

Model	Allometric1		
Equation	y = a*x^b		
Reduced Chi-Sqr	0		
Adj. R-Square	0.9884		
		Value	Standard Error
qe	a	0.52951	--
	b	1.13455	--

(c) Carbamazepine

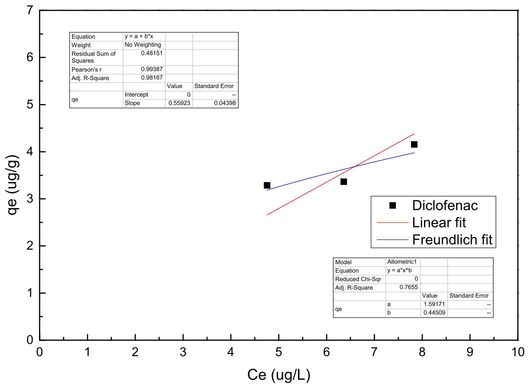

Equation	y = a + b*x		
Weight	No Weighting		
Residual Sum of Squares	0.48151		
Pearson's r	0.99387		
Adj. R-Square	0.98167		
		Value	Standard Error
qe	Intercept	0	--
	Slope	0.55923	0.04398

Model	Allometric1		
Equation	y = a*x^b		
Reduced Chi-Sqr	0		
Adj. R-Square	0.7655		
		Value	Standard Error
qe	a	1.59171	--
	b	0.44509	--

(d) Diclofenac

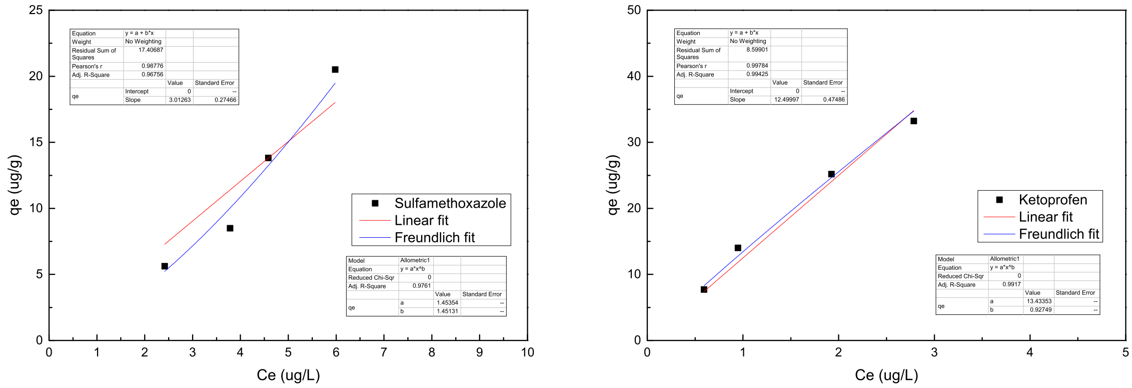

Equation	y = a + b*x		
Weight	No Weighting		
Residual Sum of Squares	17.40687		
Pearson's r	0.98776		
Adj. R-Square	0.96756		
		Value	Standard Error
qe	Intercept	0	--
	Slope	3.01263	0.27466

Model	Allometric1		
Equation	y = a*x^b		
Reduced Chi-Sqr	0		
Adj. R-Square	0.9761		
		Value	Standard Error
qe	a	1.45354	--
	b	1.45131	--

Equation	y = a + b*x		
Weight	No Weighting		
Residual Sum of Squares	8.59901		
Pearson's r	0.99784		
Adj. R-Square	0.99425		
		Value	Standard Error
qe	Intercept	0	--
	Slope	12.49997	0.47486

Model	Allometric1		
Equation	y = a*x^b		
Reduced Chi-Sqr	0		
Adj. R-Square	0.9917		
		Value	Standard Error
qe	a	13.43353	--
	b	0.92749	--

(e) Sulfamethoxazole

(f) Ketoprofen

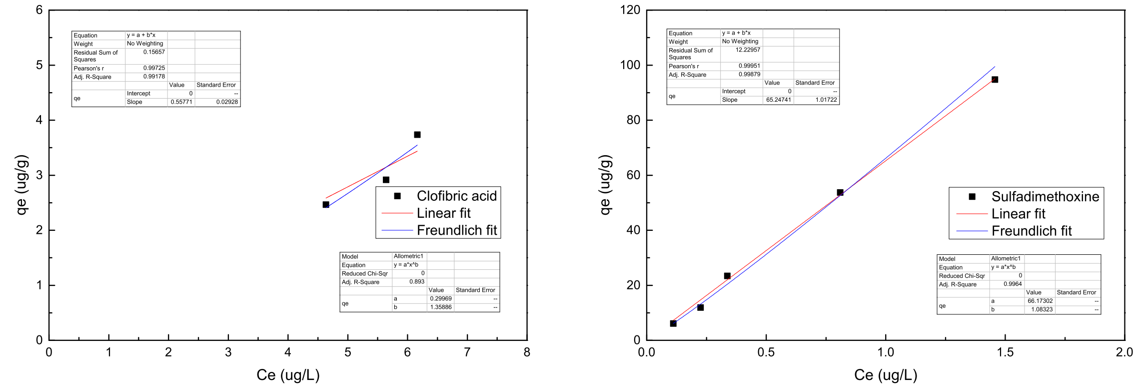

Equation	y = a + b*x		
Weight	No Weighting		
Residual Sum of Squares	0.15657		
Pearson's r	0.99725		
Adj. R-Square	0.99178		
		Value	Standard Error
qe	Intercept	0	--
	Slope	0.55771	0.02928

Model	Allometric1		
Equation	y = a*x^b		
Reduced Chi-Sqr	0		
Adj. R-Square	0.893		
		Value	Standard Error
qe	a	0.29969	--
	b	1.35886	--

Equation	y = a + b*x		
Weight	No Weighting		
Residual Sum of Squares	12.22957		
Pearson's r	0.99951		
Adj. R-Square	0.99879		
		Value	Standard Error
qe	Intercept	0	--
	Slope	65.24741	1.01722

Model	Allometric1		
Equation	y = a*x^b		
Reduced Chi-Sqr	0		
Adj. R-Square	0.9964		
		Value	Standard Error
qe	a	66.17302	--
	b	1.08323	--

(g) Clofibric acid

(h) Sulfadimethoxine

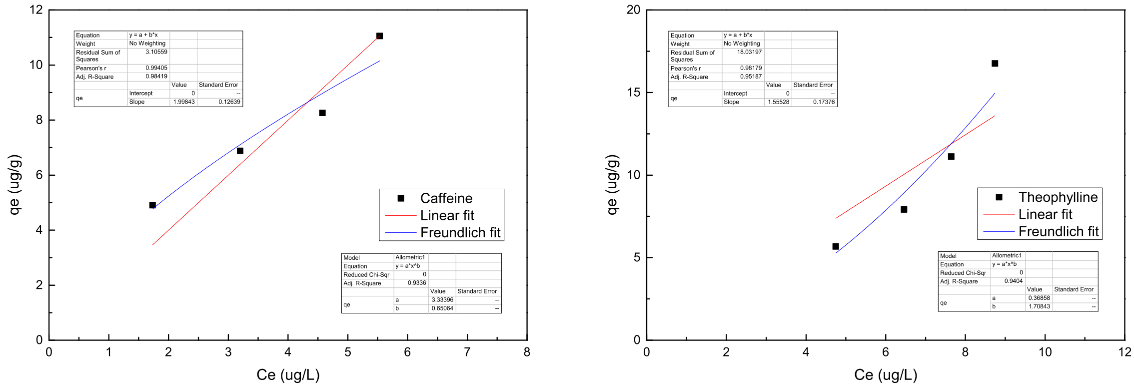

Equation	y = a + b*x		
Weight	No Weighting		
Residual Sum of Squares	3.10559		
Pearson's r	0.99405		
Adj. R-Square	0.98419		
		Value	Standard Error
qe	Intercept	0	--
	Slope	1.99843	0.12639

Model	Allometric1		
Equation	y = a*x^b		
Reduced Chi-Sqr	0		
Adj. R-Square	0.9336		
		Value	Standard Error
qe	a	3.33396	--
	b	0.65064	--

Equation	y = a + b*x		
Weight	No Weighting		
Residual Sum of Squares	18.03197		
Pearson's r	0.98179		
Adj. R-Square	0.95187		
		Value	Standard Error
qe	Intercept	0	--
	Slope	1.55528	0.17376

Model	Allometric1		
Equation	y = a*x^b		
Reduced Chi-Sqr	0		
Adj. R-Square	0.9404		
		Value	Standard Error
qe	a	0.36858	--
	b	1.70843	--

(i) Caffeine

(j) Theophylline

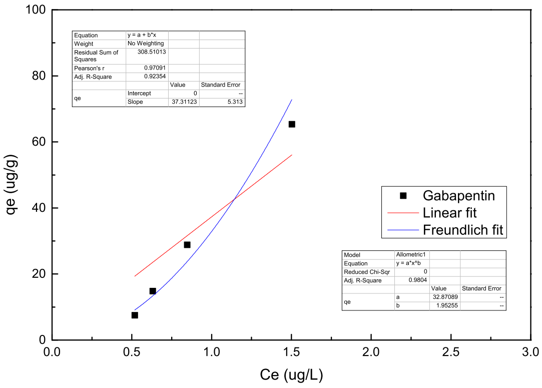

Equation	y = a + b*x		
Weight	No Weighting		
Residual Sum of Squares	308.51013		
Pearson's r	0.97091		
Adj. R-Square	0.92354		
		Value	Standard Error
qe	Intercept	0	--
	Slope	37.31123	5.313

Model	Allometric1		
Equation	y = a*x^b		
Reduced Chi-Sqr	0		
Adj. R-Square	0.9804		
		Value	Standard Error
qe	a	32.87089	--
	b	1.95255	--

(k) Gabapentin

Figure B.1: Adsorption isotherms in DW fitted by Linear and Freundlich models

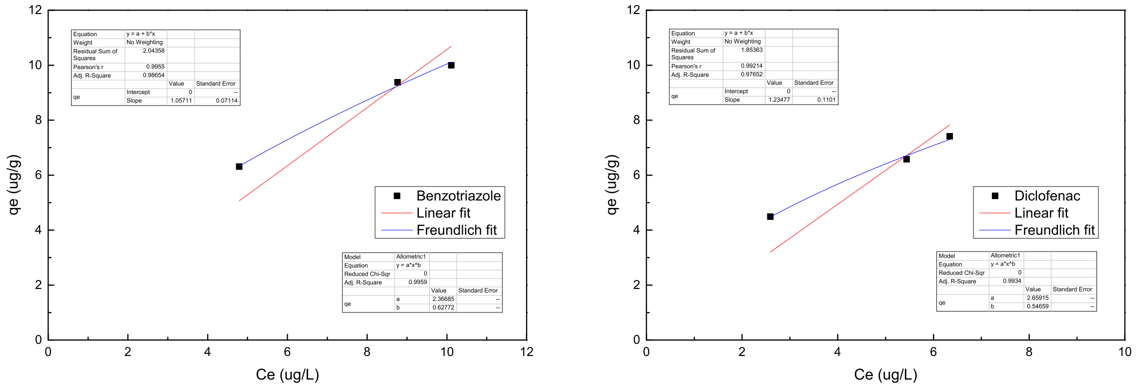

(a) Benzotriazole (b) Diclofenac

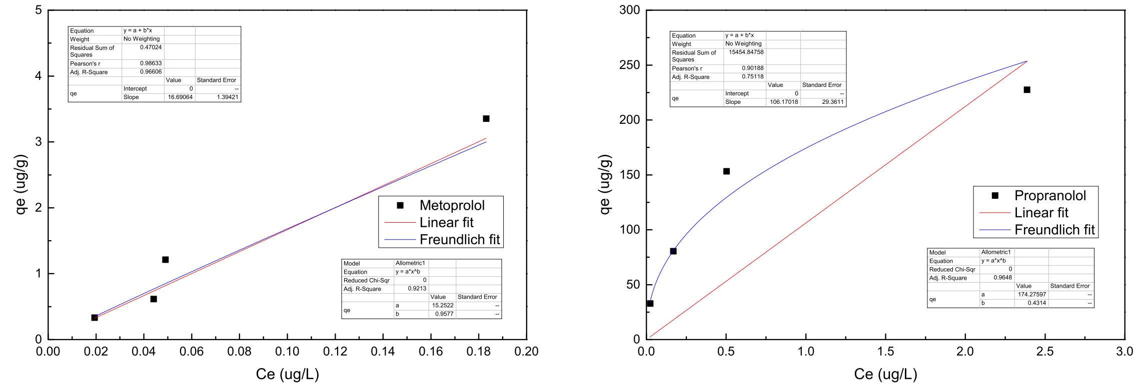

(c) Metoprolol (d) Propranolol

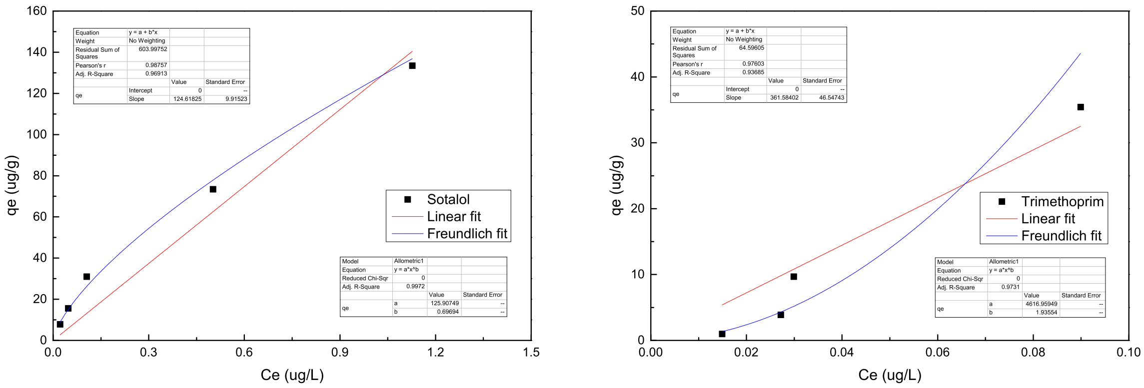

(e) Sotalol (f) Trimethoprim

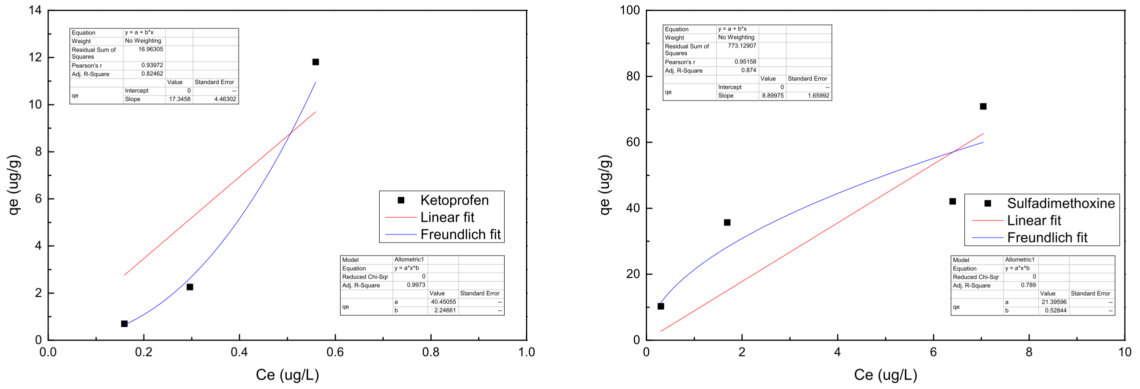

(g) Ketoprofen (h) Sulfadimethoxine

Figure B.2: Adsorption isotherms in WW fitted by Linear and Freundlich models

C

Adsorption kinetics fitted by PFO model

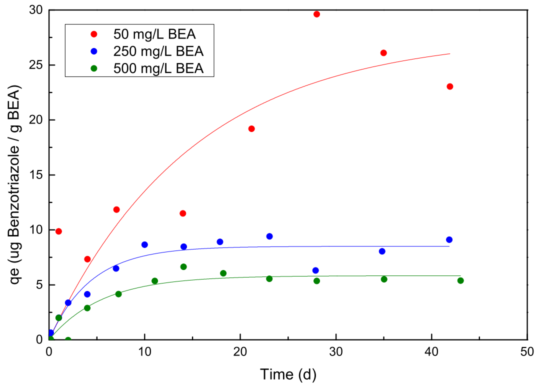

(a) Benzotriazole

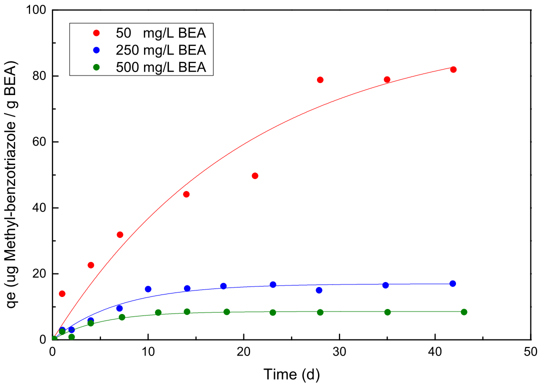

(b) Methyl-benzotriazole

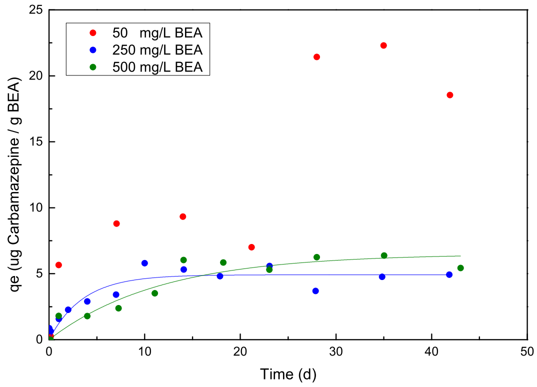

(c) Carbamazepine

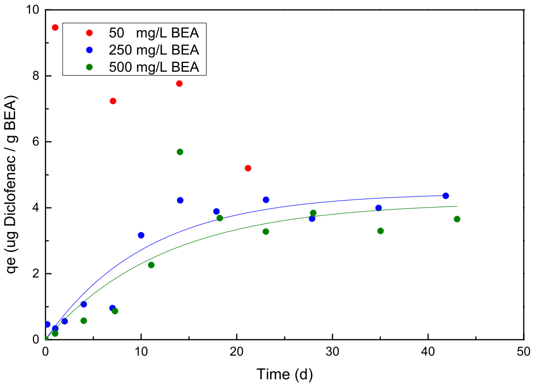

(d) Diclofenac

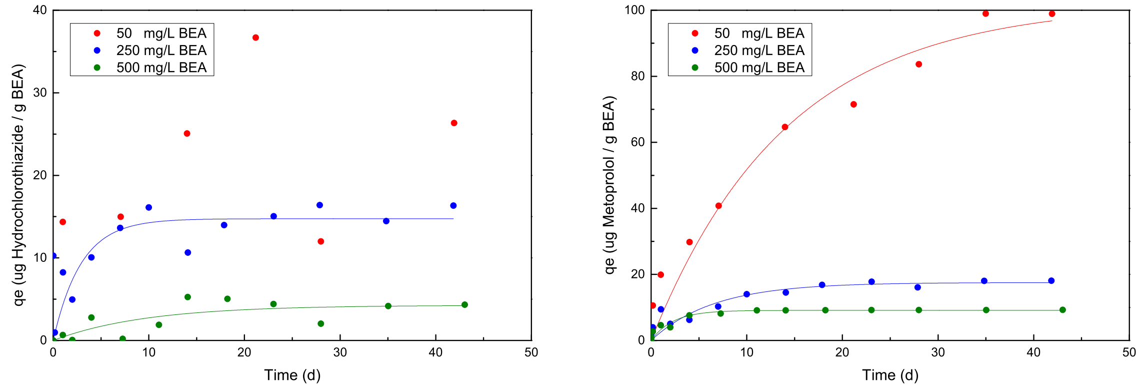

(e) Hydrochlorothiazide

(f) Metoprolol

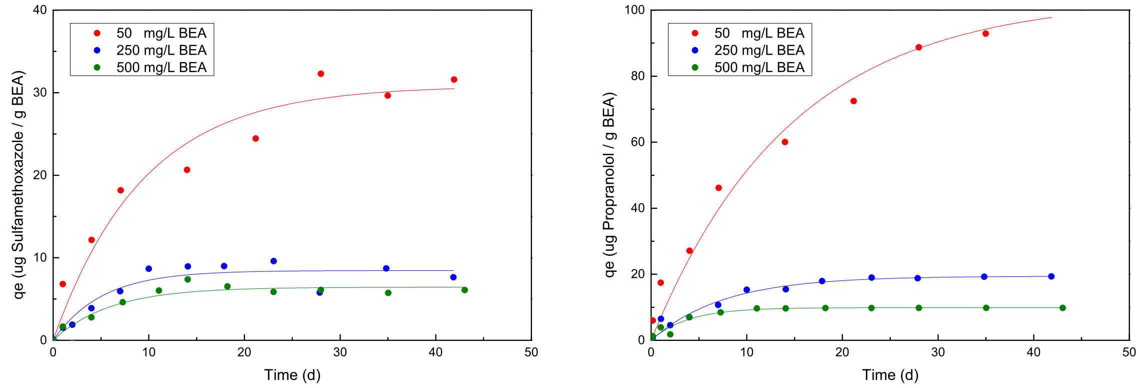

(g) Sulfamethoxazole

(h) Propranolol

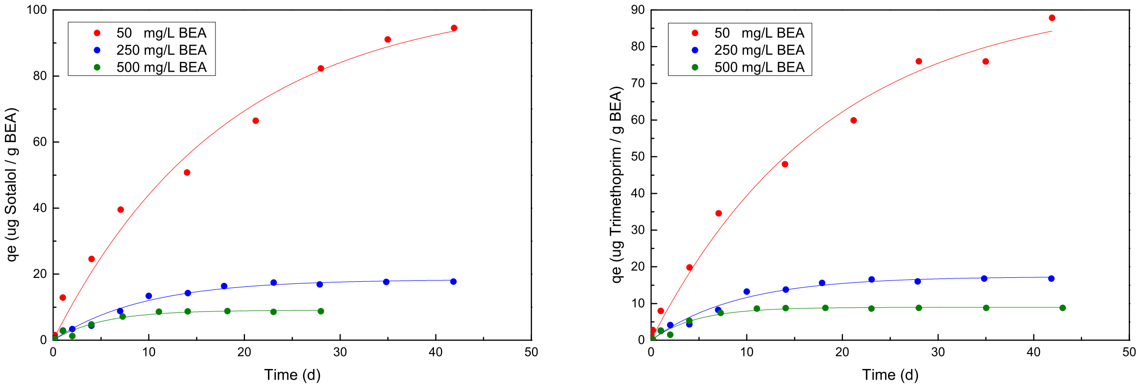

(i) Sotalol

(j) Trimethoprim

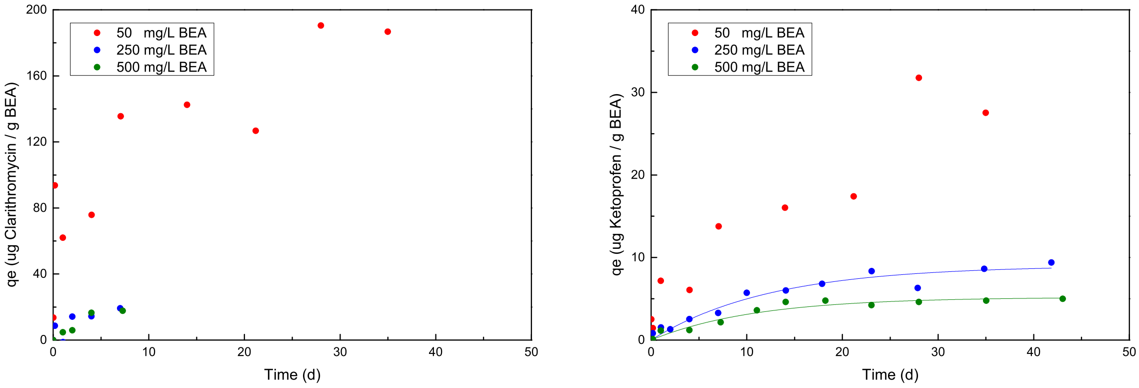

(k) Clarithromycin

(l) Ketoprofen

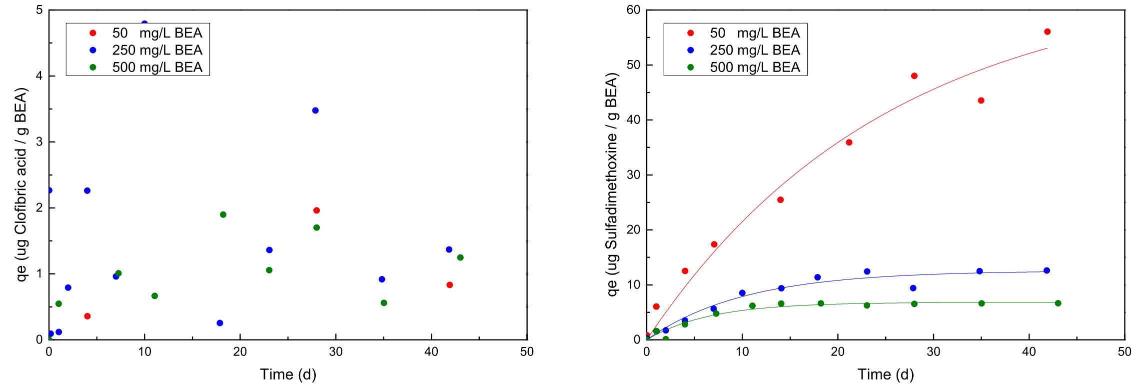

(m) Clofibric acid (n) Sulfadimethoxine

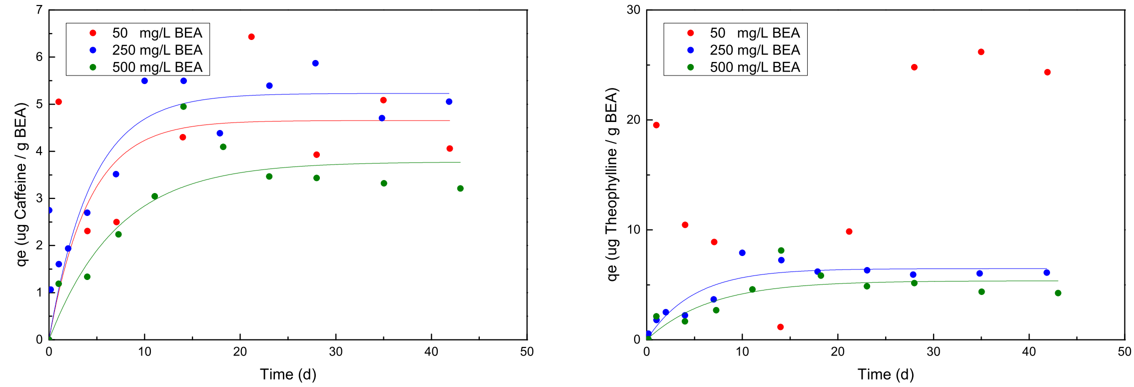

(o) Caffeine (p) Theophylline

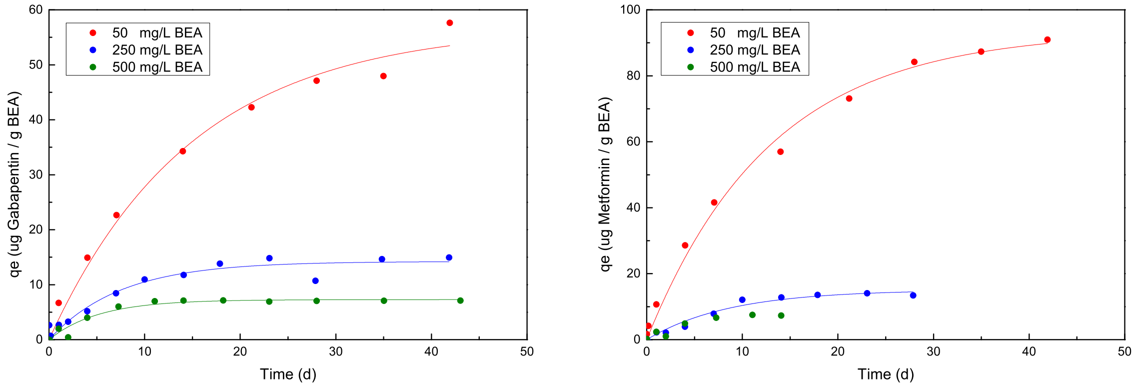

(q) Gabapentin (r) Metformin

Figure C.1: Adsorption kinetics in DW fitted by PFO model

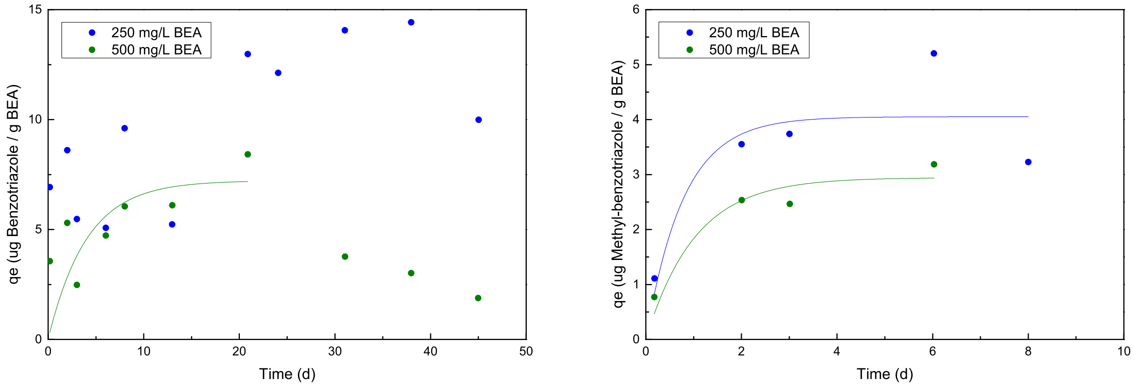

(a) Benzotriazole

(b) Methyl-benzotriazole

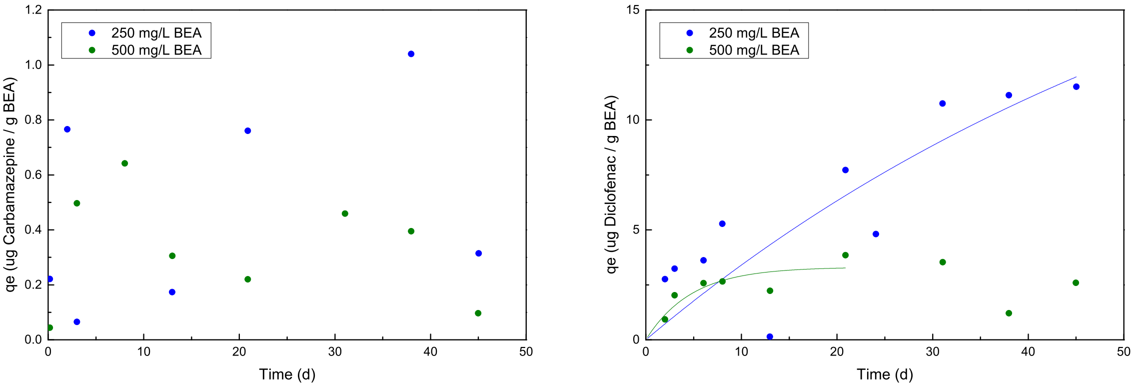

(c) Carbamazepine

(d) Diclofenac

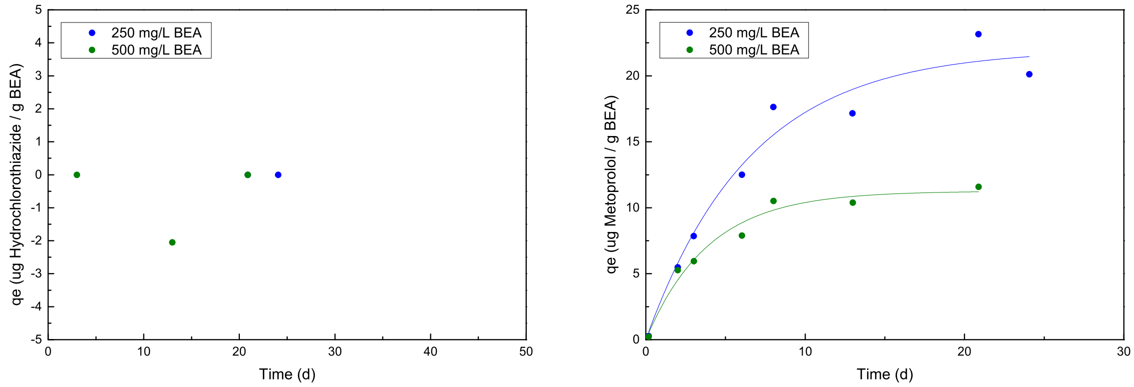

(e) Hydrochlorothiazide

(f) Metoprolol

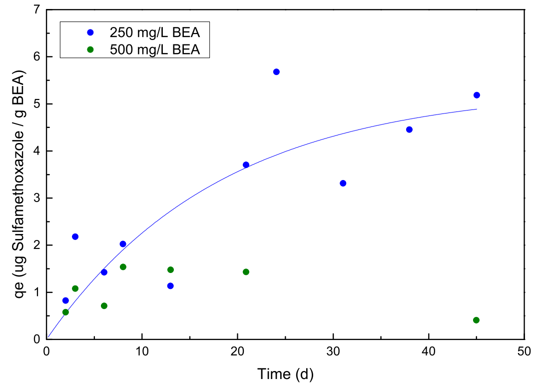

(g) Sulfamethoxazole

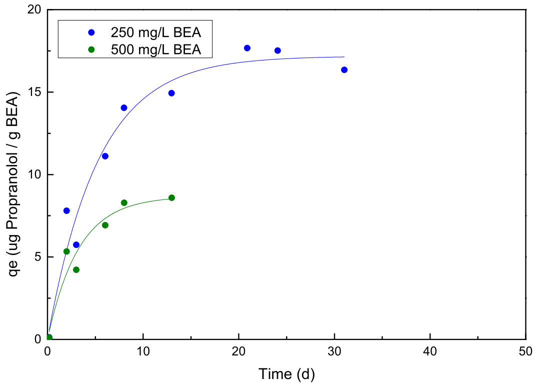

(h) Propranolol

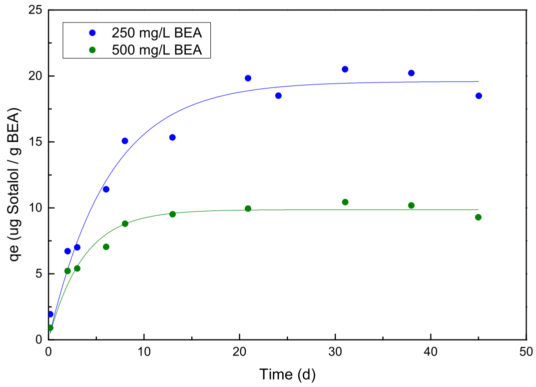

(i) Sotalol

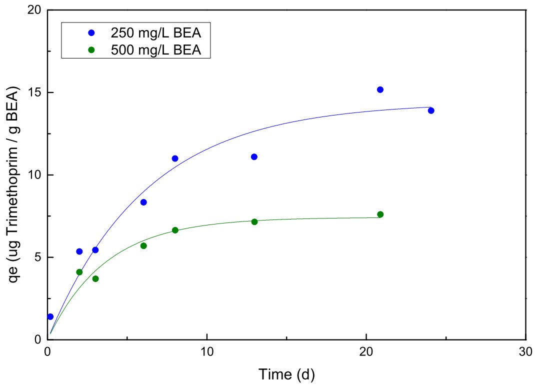

(j) Trimethoprim

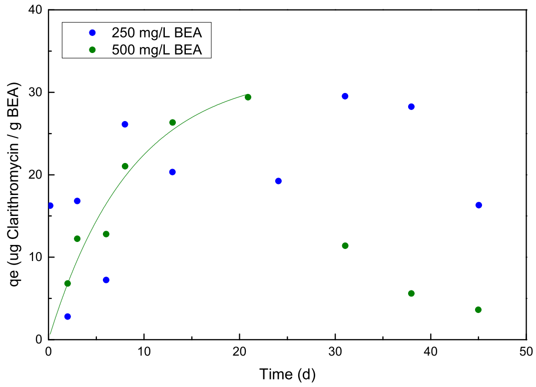

(k) Clarithromycin

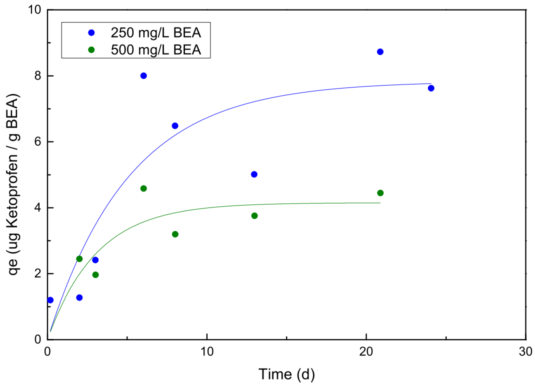

(l) Ketoprofen

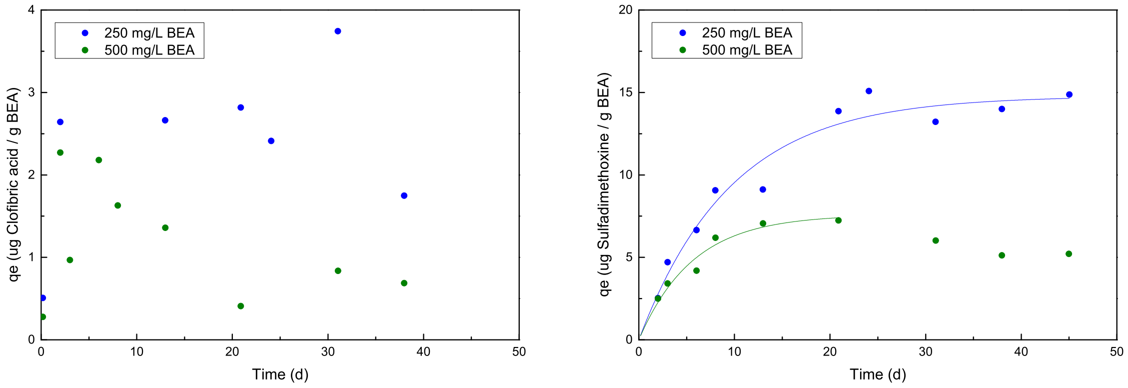

(m) Clofibric acid

(n) Sulfadimethoxine

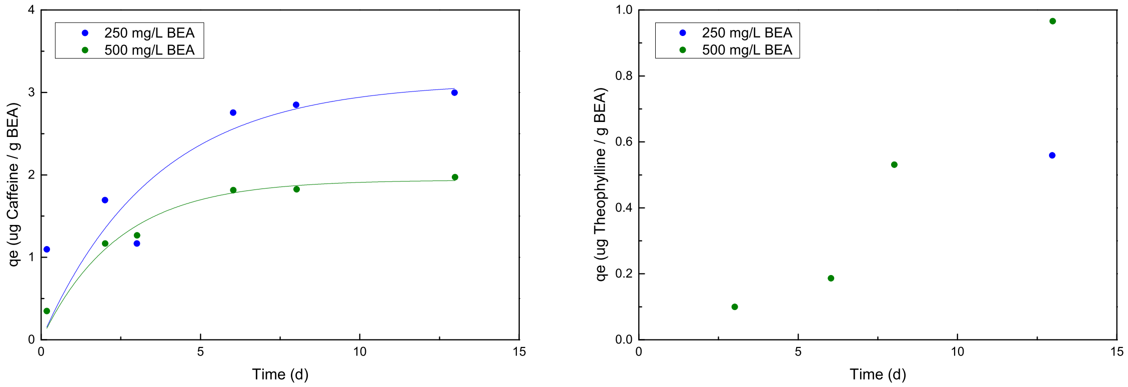

(o) Caffeine

(p) Theophylline

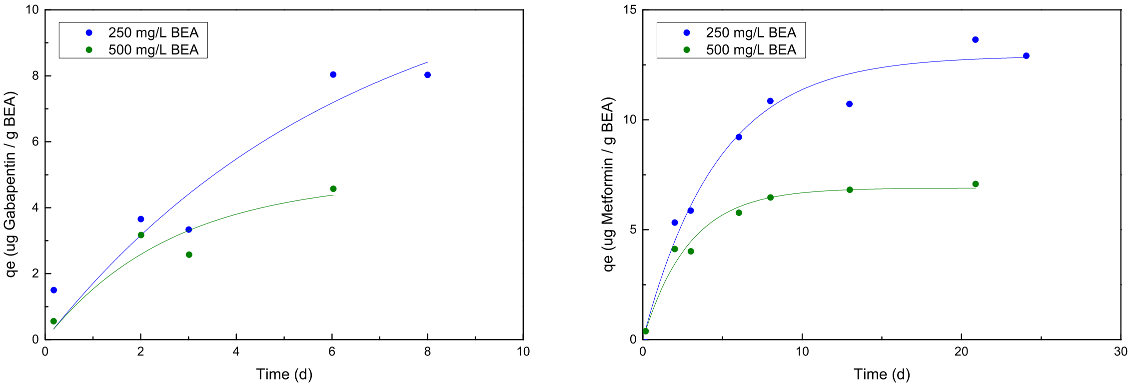

(q) Gabapentin

(r) Metformin

Figure C.2: Adsorption kinetics in WW fitted by PFO model

D

DOC, UV and ion concentration in kinetics

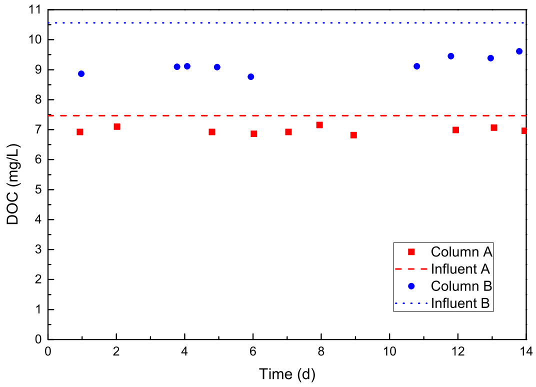

(a)

Figure D.1: DOC in kinetics

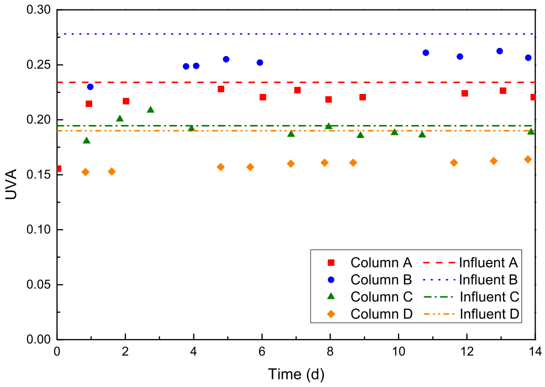

(a)

Figure D.2: UV-254 in kinetics

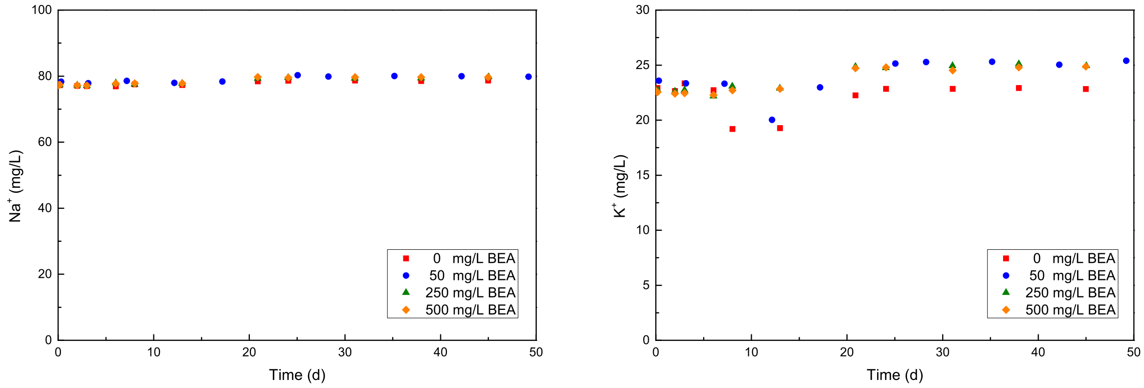

(a) Na$^+$ (b) K$^+$

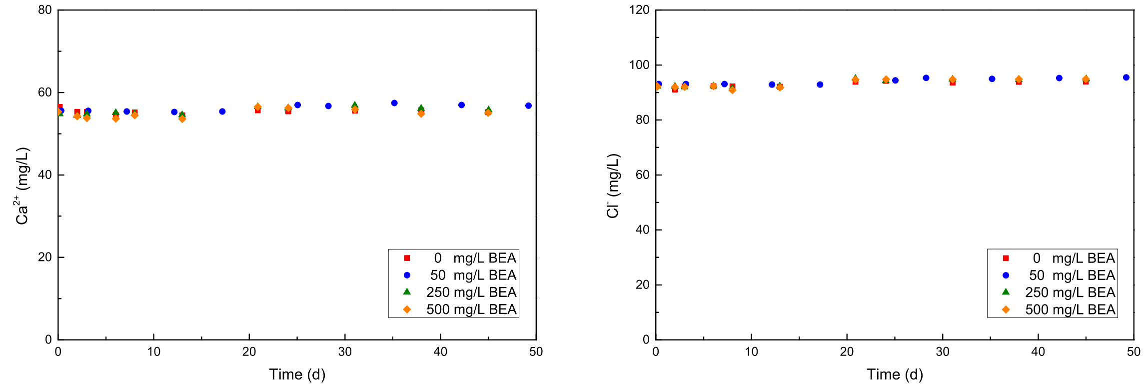

(c) Ca^{2+} (d) Cl$^-$

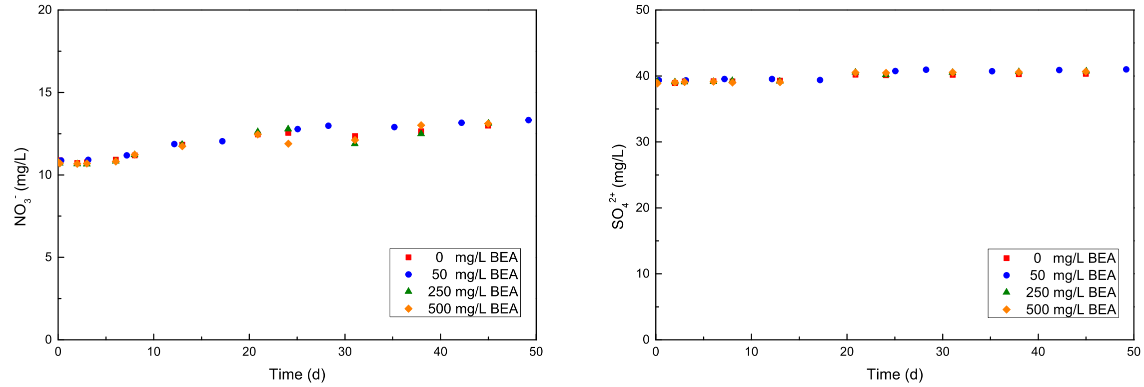

(e) NO$_3^-$ (f) SO$_4^{2-}$

Figure D.3: Ion concentration in kinetics